AN ABSTRACT OF THE PAPER OF

David Holtan Lysne for the degree of Master of Forestry in

Forest Engineering presented on May 28, 1980. Title: A

Study of Soil Disturbance and Compaction Resulting from the Use of

Ground-Based Logging Vehicles in the Sierra Nevada.

Abstract Approved: ______________________
John E. O'Leary

Some results of a study conducted in the Sierra Nevada Mountains west of Lake Tahoe are reported. The study measured soil impacts resulting from the use of a Caterpillar Tractor model D6D, a John Deere wheeled skidder model JD-640, and an FMC Corporation model FMC 210CA logging vehicle. The three vehicles were operated under carefully controlled conditions on straight 30.48 meter (100 feet) by 3.66 meter (12 feet) test strips. Three test strips were established for each machine on four sites to permit an analysis of the impacts of the machines through a range of soil moisture contents and soil types. Measurements of soil compaction were made after 1, 3, 6, 10, 15, and 20 passes with a load of logs through the test strip followed by a return through the test strip unloaded. Only the impacts resulting

from 20 complete trips are presented in this paper.

Two tools were tested to determine suitability for use as instruments to predict soil compaction. The Gus probe, a new tool designed for the study utilizing the energy derived from a weight falling through a constant distance to drive a 3.8 cm (1.5 in.) diameter foot into the ground, failed to generate useful predictive models. A cone penetrometer, the second tool tested, did generate a significant predictive model.

$$CD08 = 0.2631 - 0.0001022(CI6) \quad R^2 = .7339$$

where:

CD08 = the change in soil density, in g/cc, resulting from 20 trips of the logging vehicles, averaged to the 20.3 cm (8 in.) layer.

CI6 = the cone index, in kPa, required to push the cone tip to the 15.2 cm (6 in.) depth.

Graphs of soil densities attained after 20 trips by each machine for the four sites are presented along with curves depicting the change in densities. Greatest compaction resulted from the tractor on the slightly cohesive sites at depths greater than five cm (2 in.) with little differences between machines being observed at the five cm depth. Little differences in compaction were observed between machines at depths greater than five cm on the cohesionless sites. The FMC compacted the loose cohesionless five cm depth the least. The skidder compacted the dense cohesionless site the least.

Soil disturbance, defined as a combination of soil displacement and soil compaction, is quantified. The tractor displaced 1.9 times more soil than the FMC and the skidder displaced 1.2 times more soil than the FMC.

Appropriate equilibrium equations of motion are derived to quantify the pressures along the bottom of the tracks of the tractor and FMC and on the bottom of the tires of the skidder. The pressure distributions encountered in the study are presented.

A Study of Soil Disturbance and Compaction Resulting from the Use of Ground-Based Logging Vehicles in the Sierra Nevada

by

David Holtan Lysne

A PAPER

SUBMITTED TO

Oregon State University

in partial fulfillment of

the requirements for the

degree of

Master of Forestry

June, 1981

APPROVED:

____

Professor of Forest Engineering in Charge of Major

____

Head of Department of Forest Engineering

Date paper is presented May 28, 1980

Typed by Loui Hecht for David Holtan Lysne

ACKNOWLEDGEMENT

My research is part of a larger study on soil compaction, Predicting Soil Compaction on Forested Land, a cooperative agreement project (Co-operative Agreement Number 228) between Oregon State University's Department of Forest Engineering and the U.S.D.A. Forest Service's Pacific Northwest Forest and Range Experiment Station and the Forest Service's Missoula Equipment Development Center. A study team composed of Mr. Ben Lowman, Dr. John Sessions, Mr. Don Studier, Mr. Robert Meurisse, Mr. Gerald Anderson, Mr. J. C. Schwarzhoff, Mr. Ron Iff, Mr. La Moure Besse and Dr. Henry A. Froehlich developed the general goal for the study. Dr. Froehlich, Oregon State University, Department of Forest Engineering, was designated Project Leader. I am grateful to the study team and Dr. Froehlich for the opportunity to participate in the project.

The study was conducted on the Tahoe National Forest, Mr. Robert A. Lancaster, Supervisor. Mr. John Henshaw, Tahoe National Forest Logging Engineer, coordinated local Forest Service support. Dr. Earl Alexander assisted in site selection. Don Studier provided invaluable assistance in the early days of the project. My work would have been impossible without the supporting enthusiasm, research, and cooperation of Jerry Azevedo, Research Assistant, and Peter Cafferata, Graduate Research Assistant. Mr. Al Gaddini operated the logging vehicles. Ms. Mary King helped in data collection.

The three logging vehicles were provided free-of-charge by their manufacturers; Caterpillar Tractor Company, the John Deere Company, and the FMC Corporation.

TABLE OF CONTENTS

Page

LIST OF FIGURES

Figure		Page

LIST OF TABLES

A Study of Soil Disturbance and Compaction Resulting from the Use of Ground-Based Logging Vehicles in the Sierra Nevada.

INTRODUCTION

Mechanized ground-based logging vehicles are important tools for harvesting of timber, constructing firebreaks, treating logging residue, and clearing brush fields. Mechanized ground-based vehicles, however, produce a variety of impacts on the soil. Some soil disturbance may be beneficial, as is the case when soil scarification is desired for site preparation. But, most soil disturbance, including soil compaction and excessive displacement, is generally regarded as an adverse impact.

Soil displacement impacts of logging with ground-based systems are quite easily observed. Concern about the magnitude and importance of these impacts by forest managers and the public has dictated the need for scientific study. Numerous studies have quantified the effects of logging with ground-based systems on various soils with various slopes, moisture contents, and volumes per turn. The studies have not compared different skidding machines under controlled conditions to compare the effects of the different machines. Nor have any studies been structured to permit the formulation of a predictive equation relating compaction to the use of various ground-based machines.

In 1979, the U.S.D.A. Forest Service and Oregon State University initiated a study to quantify the differences between typical ground-based logging vehicles and to develop a predictive model for soil compaction resulting from the use of typical ground-based vehicles. Dr. Henry A. Froehlich was the Principal Investigator. This professional paper details certain aspects of the study.

Ground-based logging vehicles are generally placed into three categories: 1) crawler tractors with rigid undercarriages, 2) tracked vehicles with independently suspended track rollers (road wheels), and 3) articulated-frame, wheel skidders utilizing rubber tires in lieu of tracks. The three machines used in the study representing these three types of ground-based logging vehicles were, respectively, a Caterpillar Tractor model D6D, an FMC Corporation model FMC-210CA, and a John Deere model JD-640. The three models were selected because they represent the typical sizes of equipment commonly used in logging operations. They were equipped with features common to typical logging vehicles.

The study was conducted in the Sierra Nevada Mountains of eastern California, approximately 60 kilometers (40 miles) west of Lake Tahoe on the Tahoe National Forest. Four sites for testing were selected to represent a range of soil types, elevations, and vegetative covers. The soils on the four sites were chosen to be representative of soils normally encountered in forested land in the western United States.

Because the controlled conditions inherent in the study provide an excellent opportunity to study soil recovery from compaction, the four sites will be protected from further disturbance for a minimum of ten years in order to permit resampling.

The overall study may be broken into three phases: the data gathering and analysis phase, intended to generate a predictive model for soil compaction; the validation phase, during which the predictive model is tested; and the implementation phase, assuming the validation proves to be successful. The ultimate goal of the project is to reduce losses in site productivity resulting from soil compaction by providing forest managers with a model useful for predicting the compaction expected on a given soil from a specific type of machine.

LITERATURE REVIEW

Bradshaw (1979) observed that demand for timber products requires that the productivity of timber producing land be maintained. Lull (1959) observes that logging practices can adversely affect the productivity by compacting and disturbing the forest soil. Froehlich (1978a) reports that between 25 and 35 percent of an area logged by crawler tractors is in well-defined tractor skid trails. The same study also reports between 12 and 20 percent of an area logged by a low ground-pressure, tension-suspension logging vehicle is similarly disturbed. Comparable disturbance figures are not available for rubber-tired skidders. The correlation between disturbance from logging with ground-based systems and compaction has been frequently documented. Twenty years ago, Lull (1959), observed that compaction of forest soils was becoming a more serious problem as the use of heavy ground-based logging vehicles increased. Lull also observed that the extent of the compaction depended on the characteristics of the ground-based vehicles used, terrain, frequency of travel, soil types, and soil moisture content. Hatchell and others (1970) recognized that logging can cause soil compaction, puddling, and displacement, but they pointed out that compaction and disturbance of forest soils have received too little attention.

Lull (1959) defined soil compaction as, "... the packing together of soil particles by instantaneous forces exerted at the soil surface resulting in an increase in soil density through a decrease in pore space." Bell (1977) observes that if the load applied to a soil is sufficiently great to overcome the soil shear resistance, the load will sink into the soil and the soil beneath the load will be densified. The compacted soil has a higher bearing capacity than the uncompacted soil. Sinkage of the load into the soil and compaction stop when the soil bearing capacity becomes equal to the applied load. Froehlich (1974) states that the initial sinkage of a load into the soil causes soil aggregate rearrangement, thus reducing macroscopic pore space without aggregate degradation. Further pressure will result in plastic deformation of the aggregate contact points and eventual aggregate destruction. A puddled soil may result as a result of the breakdown of soil structure.

Bell (1977) also states that soils even with a moisture content dry of optimum moisture content for maximum compaction on a Proctor test, may be compacted and that increased loadings produced denser soils. Soils wet of optimum Proctor test moisture content are merely remolded with increased energy levels above a relatively low loading pressure. Bell felt that the optimum moisture content for compaction is associated with the lowest water content at which the shear resistance for a given load is overcome. Soils wet of optimum experience bearing capacity failures and remold more than compact, although some compaction does occur.

Lull (1959) reports that the higher the organic matter content in a soil, the less the compacted density for a given compactive effort and the higher the moisture content required for optimum compaction. Lull also points out that soils with a wide range of partial sizes will compact to a higher density than more uniform soils. Weaver and Jamison (1951) report that a compacted fine soil will be less dense than an equally compacted coarse soil because the relatively high micropore space in the fine soil is not destroyed in the compaction process. Hatchell and Ralston (1970) found that the more porous a soil is initially, the relatively greater the amount of compaction will result when compared with less porous soils.

The similarities in behavior of soil subjected to compaction effort in laboratory tests, such as the Proctor tests, and soils subjected to compactive loadings beneath the tires or tracks of ground-based logging vehicles has been long established.

Raghavan and others (1976) studied the effects of the operation of agricultural equipment equipped with rubber tires on agricultural soils. They found that the pattern of compaction resulting from loaded rolling tires compared well with the standard Proctor test. They felt that the compaction resulting from the agricultural equipment could best be duplicated in a laboratory by static or kneading compaction tests. They found that the maximum tire ground pressure in the field tests of 159 kPa (23.04 p.s.i.) produced significantly less compaction than the standard Proctor test and that a field tire pressure of 1724 kPa (250 p.s.i.) would be required to attain the same compaction as the standard Proctor laboratory test.

Froehlich (1974, 1978b) states that both vertical pressure and vibration lead to soil compaction. Pressure and vibration are inherent qualities of ground-based logging systems. Froehlich further reports that the soil compaction observed after logging results from a combination of pressure, kneading, vibration, and pressure from the dragging logs. Bell (1977) reports that optimum compactive efficiency is attained by operating heavy equipment with large ground contact areas, high ground pressures, and slow rates of travel if the soil is dry. If the soil is wet and the heavy equipment would suffer bearing capacity failures, lighter equipment with smaller contact areas and pressures becomes more efficient for the compaction of cohesive soils.

Lull (1959) states that the pressure beneath a track of a tracked ground-based logging vehicle may be less than beneath the tire of a wheel skidder, but the compaction may be greater beneath the track due to the effects of vibration. Lull also reports that the pressure beneath the ribs on the tires of wheeled skidders has been found to be four to five times higher than the pressures observed under ribless tires. Lull concurs with Froehlich that the ground pressure of the logs being skidded must also be considered. Weaver and Jamison (1951) found that increasing the draft on a wheeled skidding vehicle for constant vertical soil pressure increased soil compaction due to complex soil loadings resulting from tire slip. Numerous studies discussed static ground pressures of various ground-based logging vehicles, but no studies were found which addressed the problem of dynamic loaded pressures of a vehicle operated under constant velocity.

Froehlich (1974, 1978b), Hatchell and others (1970), and Lull (1959) note that greater compaction results from operating ground-based logging vehicles on wet soils than on dry soils. Weaver and Jamison (1951) found that for equal compactive efforts an unconfined soil will attain maximum compaction at a lower moisture content than the same soil compacted in a confined Proctor test.

Froehlich (1978a) found soil density increasing most during the first few trips of a tension-suspension, low ground-pressure logging vehicle, but compaction continued slowly with increased number of passes as the litter layer was removed. Steinbrenner (1955), in a study using a small crawler tractor, found little increase in soil density from six trips to ten trips. Weaver and Jamison (1951) found the greatest increases in soil density resulting from passage of a loaded rubber tire occurred in the first four of ten passes. Hatchell and others (1970) observed in a study of tree-length skidding using crawler tractors and wheeled skidders that soil bulk density increased markedly after one or two trips with a more gradual increase in bulk density as number of trips increased.

Froehlich (1978a) reports soil density increases are rarely observed below 25.4 cm (ten inches). His study bore out the previous observations. Lull (1959) reports most studies show that compaction usually does not exceed 30.5 cm (12 inches) directly below the bearing surface. Froehlich (1974) reports that compaction depth is variable and will be observed deeper under wet conditions than dry conditions and with looser soils prior to compaction than denser soils.

Pritchett (1979) observes that the majority of small roots lie in the upper 20 cm (7.9 inches) of the soil surface.

Froehlich (1978a) found 12 to 20 percent of the total surface area of skid trails for a tension-suspension, low ground-pressure, logging vehicle exhibited exposed mineral soil after 20 trips. Froehlich (1978b) also states that most soil disturbance during timber harvesting displaces the soil a relatively short distance.

The use of ground-based logging vehicles causes soil disturbance and compaction capable of adversely affecting forest timber productivity. Numerous studies were found which quantified the impacts resulting from the use of ground-based logging vehicles, but no studies provided predictive models for predicting impacts. The study detailed in this paper was initiated to generate predictive models.

SITE DESCRIPTIONS

The study was conducted on the western slope of the Sierra-Nevada Mountains in northern California on the Tahoe National Forest. The Tahoe National Forest is located immediately west and north of Lake Tahoe. Each of the four test sites were located on National Forest land ownership.

The Moonshine site is located on a broad convex ridgetop characterized by gently undulating terrain at approximately 680 meters (2225 feet) elevation above sea level. Slopes average three percent with a generally southerly aspect although test strips seven, eight, and nine had a northerly aspect. The vegetative climatic zone is mixed conifer. Precipitation averages approximately 140 cm (55 inches) per year. The soil is derived from siliceous plutonic parent material and is well-drained.

The Bullards Bar site is located on a broad ridgetop summit at 1040 meters (3400 feet) elevation. Slopes average seven percent with a southerly aspect. The soil is derived from a schist (metasediment) parent material and is well-drained. The climatic zone is classified as mixed conifer. Precipitation averages 178 cm (70 inches) per year.

The Pliocene Ridge site is located on a rounded broad ridgetop at an elevation of 1510 meters (4950 feet). The test strips slope westerly at five percent. The vegetative climatic zone is mixed conifer. Average annual precipitation is 152 cm

(60 inches) per year. The soil is well-drained and is derived from andesitic lahar parent material.

The Yuba Pass site is located immediately west of the ridgeline of a narrow periglacial mountain slope. The slopes of the test strips average ten percent with a westerly aspect. The elevation is 2180 meters (7150 feet), the highest elevation of the four sites. Precipitation averages 152 cm (60 inches) per year. The vegetative climatic zone is red fir (*Abies magnifica* [A. Murr.]). The soil is well-drained and is derived from a granodiorite parent material.

VICINITY MAP

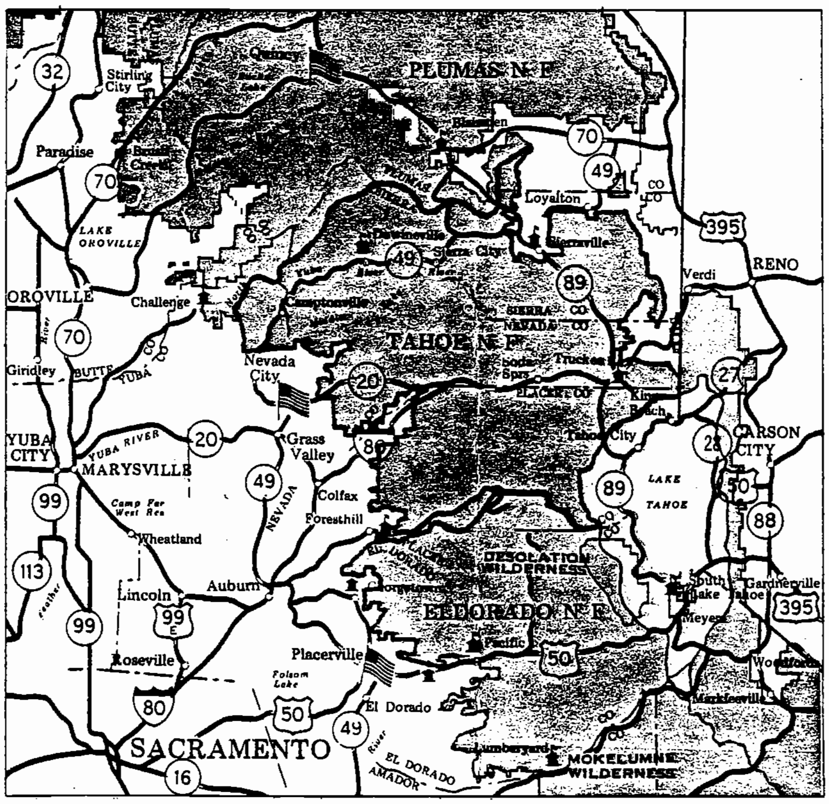

Figure 1. Location of Study Area.

TABLE I. SUMMARY OF SOIL PARTICLE SIZE AND ATTERBERG LIMITS ANALYSIS.

	Moonshine	Bullards Bar	Pliocene Ridge	Yuba Pass
Coarse Fragments, over 6.35 mm (0.25 inch) Diameter, Percent	0	11	32	18
Sand, Percent[1]	62	39	52	70
Silt, Percent[1]	24	29	13	10
Clay, Percent[1]	14	21	3	2
Liquid Limit, % M.C.	38.6	58.2	-	-
Plastic Limit, % M.C.	34.9	52.6	NP[2]	NP[2]
Plasticity Index, % M.C.	3.7	5.6	NP[2]	NP[2]
U.S.D.A. Soil Classification	Sandy Loam	Loam	Loamy Sand	Loamy Sand
Unified Soil Classification	ML	MH	SM	SM

[1] Sand sized particles range from 2.0 to 0.05 mm diameter
Silt sized particles range from 0.05 mm to 0.002 mm diameter
Clay sized particles are smaller than 0.002 mm diameter

[2] NP = Non-plastic

STUDY DETAILS

TEST STRIPS AND PLOTS

Nine test strips were located on each of the four sites. The nine strips allowed three strips for each of the three machines used to permit skidding with varying soil moisture contents. The goal was to test the effect of logging equipment operating on soils below optimum moisture content, close to optimum moisture content, and above optimum moisture content as determined by the Standard AASHTO Proctor Test, ASTM D-698-70. The sites were selected so that the nine test strips were in close proximity to each other over a relatively constant slope, with sufficient room for return routes for the equipment, and for log storage areas.

Sites were selected which had very low slopes. The maximum slope for all skid trails was 14 percent. The strips at each site were also located to avoid excessive accumulations of rotting forest debris, standing trees, or prior disturbance.

Each strip at every site was staked with engineering lath 30.48 meters (100 feet) long by 3.66 meters (12 feet) wide. Strips were located as straight as possible. Sufficient room was allowed at each end of the strips to permit the machine and turn of the logs to enter and exit the strip aligned with the strip while maintaining constant velocity. Within the strips, all standing trees were removed and the resulting stumps cut off as close to the ground as possible to reduce fluctuations in machine speed, direction, or soil loading. Large logs were removed, but smaller litter and logs were left in the strips. Care was taken to ensure that each strip for a given site was covered with equal amounts of loose surface litter and small down trees. Loose surface litter was removed or added as required to obtain nearly constant amounts for all strips on a site. The quantity of loose litter was not constant between sites, however, because the amount of litter is a reflection of the soil, vegetation, and climate at that site. Profile development at the site may also be correlated to litter. Analysis of the effects of machine type and number of passes was simplified by reducing the possible variation in the independent soil variables and machine speed. Within the 30.48 meter by 3.66 meter strip, a strip segment 14.63 meters (48 feet) long by 3.66 meters (12 feet) wide was located. Density measurements were made within this smaller segment to eliminate as much fluctuation in machine speed and soil properties as possible. The 14.63 meter test plot was split into two shorter plots if necessary to ensure uniformity. The two sub-plots would have a total length of 14.63 meters. The test segment was divided into 64 plots, 0.91-meter (3 feet) by 0.91-meter squares. From the 64 plots, ten were selected randomly for density measurements. The test plot was referenced in direction and length to survey hubs driven into nearby standing reference trees for possible future remeasurements. Thus, location of the original ten measurement plots can be re-established to analyze the soil recovery from compaction with time. The same ten measurement squares were used throughout the testing for each strip. To further reduce any variation in soil compaction with number of passes, the same holes for the neutron probe were used if the original holes would be relocated. With few exceptions, the same holes were able to be relocated throughout the testing process.

Profiles were taken at right angles to the strip to obtain soil profiles before and after treatment. The profile location was not randomly selected, but was located to avoid stumps or excessive trail uneveness. Equal elevation hubs were established on either side of the trail at right angles to the trail in close proximity to the ground level. By tightly stretching a cloth tape between the hubs, the vertical distance to the litter and soil surface could be established consistently from a known datum before and following skidding. All obvious breaks in the micro-terrain were recorded.

EQUIPMENT SELECTION

Three general types of machines, a rubber-tired skidder, a crawler tractor, and a high speed track vehicle with independently suspended road wheels were selected for use in the tests. These machines represent the basic ground-based logging vehicles commonly encountered in ground skidding logging operations. All vehicles were equipped with skidding arches to ensure a slight elevation of the leading end of the log. The sizes of the machines chosen were to represent common sizes for the vehicles as used in log skidding operations.

The rubber-tired skidder class included machines which weigh between 6800 kilograms (15,000 pounds) and 11,340 kg (25,000 lbs.), have between 74.57 kilowatts (100 horsepower) and 104.40 kW (140 hp) net engine power.

The actual machine used in the tests was a John Deere model JD640 skidder. The skidder's weight, as determined for the actual machine used in the tests, was 9063 kg (19,980 lbs.). Net engine power is listed 83 kW (110 hp). The tire size of the vehicle used in the tests was 23.1 x 26, inflated to 138 kPa (20 psi) cold pressure. As measured in the field in loose soil, the ground surface contact area was 3381 square centimeters (524 square inches) per tire with the tire ribs embedded in the ground, but the flat rubber surface on top of the soil. The skidder was equipped with a decking blade. Wheel weights were not used.

The crawler tractor class was represented by machines which weigh approximately 13610 kg (30,000 lbs.) with approximately 104 kW (140 hp) net engine power. The tractor was to have 45.7 cm (18 inches) wide tracks. The length of the track in contact with the ground was not specified.

The actual machine used was a Caterpillar tractor model D6D. The specific vehicle used in the tests weighed 17,800 kg (39,240 lbs.), had 50.8 cm (20 in.) wide tracks with a ground contact length of 269.2 cm (106 in.), and a net engine power of 104 kW (140 hp). The vehicle was equipped with a model 65 blade and an integral arch.

The high speed, independently suspended, track roller vehicle specified for use in the tests is manufactured by the FMC Corporation. Because only one manufacturer produces high speed independently suspended, track roller vehicles for use in the logging industry, the manufacturer was specified. The specific machine used in the tests was an FMC model 210CA. The engine is rated at 149 kW (200 hp) net power. The specific vehicle used in the test weighed 13,354 kg (29,440 lbs.). The vehicle's tracks were 55.9 cm (22 in.) wide and had a ground contact length of 287.0 cm (113 in.). The vehicle was equipped with a standard decking blade.

Turn weights were planned to equal approximately 80% of the effective drawbar pull, or 3630 kg (8,000 lbs.) for the rubber-tired skidder and 6800 kg (15,000 lbs.) for both the crawler tractor and the FMC. The drawbar pull was determined based on typical skidding speeds and gear. The turn weights were felt to be appropriate according to the equipment operator who experimented with various turn weights outside of the testing area prior to the first testing period. The turn weights permitted acceptable machine speed and handling characteristics. Due to the uncertainties inherent in estimating wood densities, the turn log weights had to be estimated prior to commencing the testing. Scheduling difficulties precluded weighing the logs prior to commencing testing for each site. Actual log weight was determined by weighing both ends of the log. Care was taken to ensure that the chain and scale supporting one end of the log hung vertically, thereby eliminating any horizontal component on the log in order to simplify calculating the log center of gravity. Once logs were obtained for each machine for each site, the logs were numbered and the same logs were used throughout the testing. The crawler tractor and the FMC used the same logs for each site. One log turns were avoided for the rubber-tired skidder because one log turns of sufficient weight were not possible for the crawler tractor or FMC and because one log turns are not common. The large end of the log was typically chokered and the turns were skidded with the leading end of the logs slightly suspended. The FMC carrier arch was fully retracted while skidding with the large end of the logs supported by the arch bunk. The log weights by machine and site are summarized in Table II.

SOIL TESTING PROCEDURE

Density was determined during testing by using a double probe stratagage manufactured by Campbell Pacific Nuclear Corporation. The double probe feature permits determination of soil density for a specific depth without destructive sampling. In using the nuclear probe, both the neutron source probe and the probe housing the Geiger-Mueller tube are inserted into the ground to the selected depth at a constant spacing of 30.48 cm (12 in.). A display on the top of the probe indicates the number of impulses generated by the Geiger-Mueller tube as a result of the energy transmitted through the soil. The denser the material through which the radiation must pass in travelling from the source to the receptor, the lower the count indicated on the display. One-half minute counts were used exclusively to determine soil density. Two counts were taken at each density sample depth. Additional counts were

TABLE II. SUMMARY OF TURN WEIGHTS.

SITE	TOTAL WEIGHT, BY LOG kg	TOTAL WEIGHT, BY LOG lbs	MACHINE
Moonshine	2,990	6,590	
	2,055	4,530	
	1,465	3,230	
	900	1,985	
TOTAL	7,410	16,335	Tractor, FMC
	2,055	4,530	
	1,465	3,230	
	900	1,985	
TOTAL	4,420	9,745	Skidder
Bullards Bar	1,880	4,140	
	3,235	7,130	
	1,590	3,510	
TOTAL	6,705	14,780	Tractor, FMC
	1,880	4,140	
	1,590	3,510	
TOTAL	3,470	7,650	Skidder
Pliocene Ridge	1,785	3,930	
	2,165	4,770	
	1,125	2,480	
	710	1,560	
TOTAL	5,785	12,740	Tractor, FMC
	1,125	2,480	
	1,630	3,590	
TOTAL	2,755	6,070	Skidder
Yuba Pass	3,205	7,070	
	1,040	2,290	
	1,565	3,450	
TOTAL	5,810	12,810	Tractor, FMC
	635	1,405	
	1,040	2,290	
	1,565	3,450	
TOTAL	3,240	7,145	Skidder

taken if the two initial counts were not judged sufficiently close due to the inherent random nature of the flow of neutrons. Additional readings were taken until two readings agreed closely. All gage counts were used to estimate soil density, excepting obvious outliers.

The readings were averaged and divided by a standard count to obtain a ratio. The standard count was determined for each nuclear probe twice daily, or more frequently if in the opinion of the operator the probe was performing erratically. A standard count consists of averaging ten readings of one-quarter minute duration on the gage when it is situated on a standard block of uniform density. The ratio of the field count to the standard count would be entered into a regression equation for each probe to obtain a point estimate for wet density. A regression equation was derived for each probe by loading a box of known volume with soils of known weight, computing density from the known weight/volume relationship, and regressed against the ratio obtained by the probe as discussed previously. The coefficients of determination obtained for the nuclear probes in this manner were 0.99 at all depths. The wet density values obtained with the stratagages were converted to dry density after soil moisture content was determined by gravimetric methods.

Gravimetric moisture content samples were taken from each nuclear probe plot within 30.48 cm (12 in.) of the nuclear probe holes for the 0 to 15.24 cm (0-6 in.) depth range and the 15.24

to 30.48 cm (6-12 in.) depth range prior to commencing skidding operations and for the same depth ranges between the nuclear probe holes following skidding operations. Tests showed that there was no significant difference between the beginning and ending moisture content, nor between the 0 to 15.24 cm and 15.24 to 30.48 cm depths. Thus, moisture content used for the specific sample plot for the determination of dry density from wet density was the average of all four moisture contents for each plot.

Measurements with the nuclear probe were taken at the ten randomly located sampling squares after 0, 1, 3, 6, 10, 15, and 20 round trips. One round trip consisted of a pass downslope with the turn of logs followed by one pass upslope without the turn of logs. For convenience, all loaded passes were made, the logs were dropped, and then all unloaded passes were made for each sampling interval prior to measuring densities. Soil density measurements were made at 5.08, 10.16, 15.24, 20.32, and 30.48 cm (2, 4, 6, 8, and 12 in., respectively) depths on each sample square and at significant terrain breaks along the profile for measuring soil disturbance following all 20 trips.

Cone penetrometer measurements were taken prior to commencing skidding operations. The measurements were taken in accordance with the procedures outlined in ASAE R313.1 from a litter-free soil surface although some of the penetrometer operators experienced some difficulty in maintaining the constant rate of penetration

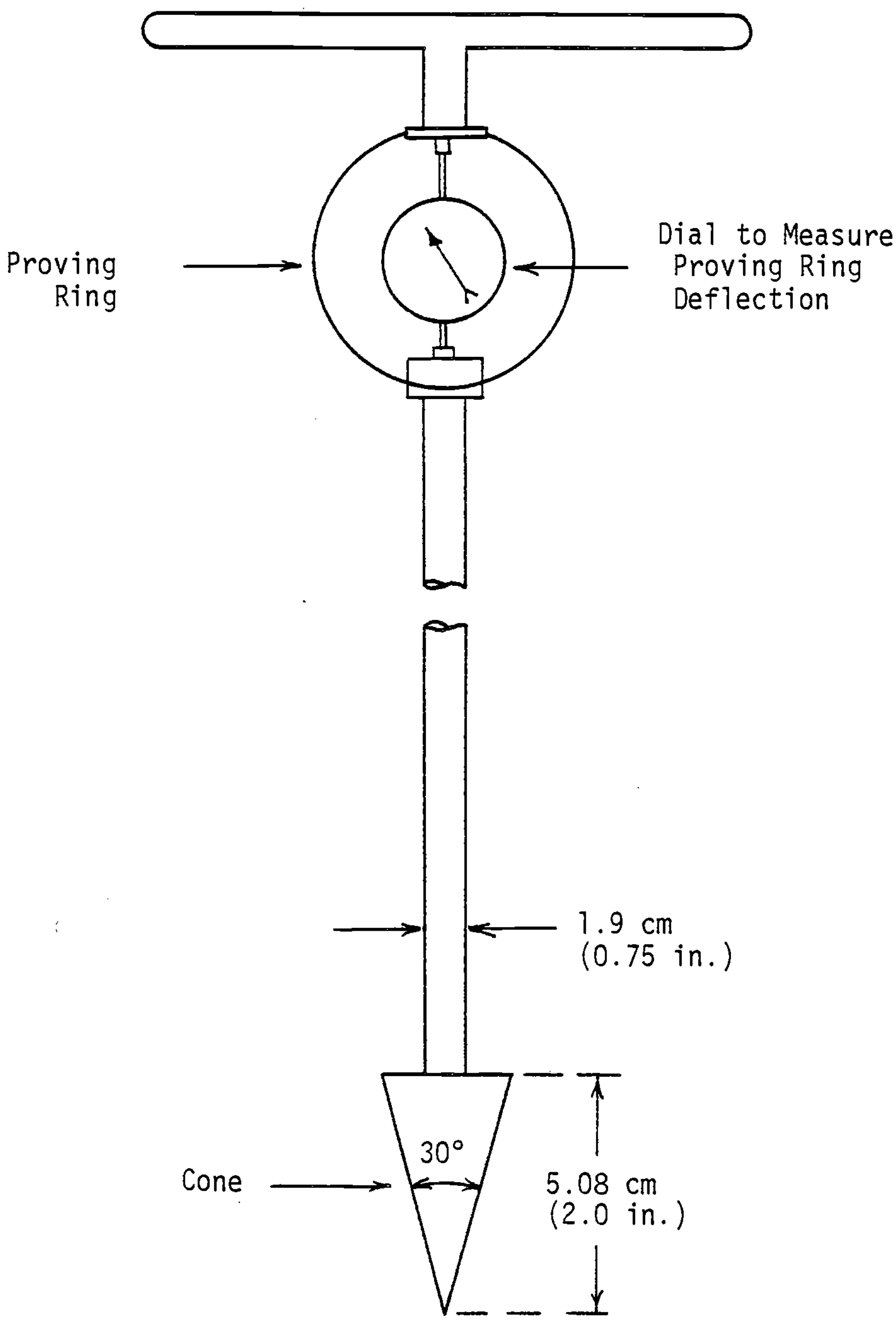

Figure 2. Cone Penetrometer.

desired. The cone penetrometer had a 5.82 cm^2 (0.902 $in.^2$) base area and a 1.91 cm (0.75 in.) diameter shaft. The penetrometer dimensions are those normally associated with use on very soft, loose soils. Cone penetrometer measurements were taken at random locations within the 14.63 meter by 3.66 meter test plot if sufficient time was available to make the measurements prior to commencing testing. If sufficient time was not available, the penetrometer readings were taken immediately outside the test strip, but in close proximity to the test strip. Ten cone penetrometer readings were taken at total penetration depths of 10.2 cm (4 in.) and 15.2 cm (6 in.). The 10.2 cm and 15.2 cm penetrations correspond to 5.1 cm (2 in.) and 10.2 cm (4 in.) penetrations measured from the point at which the base of the cone is flush with the soil surface. The depths used to test the predictive quality of cone penetrometer readings for estimating ultimate compaction were the 10.2 cm and 15.2 cm total penetration depths. Cone index is defined in ASAE R313.1 as the force per unit basal area required to push the penetrometer cone to a given depth. An independent set of calibration measurements were made with the cone penetrometer. The penetrometer dial readings were regressed against pressure to produce the calibration curve given in Appendix A.

A new tool was designed by the author and George Bradshaw, logging engineer, U.S.D.A. Forest Service, to attempt to predict ultimate compaction resulting from the use of ground-based equipment. The tool incorporates a weight dropped along a shaft through a

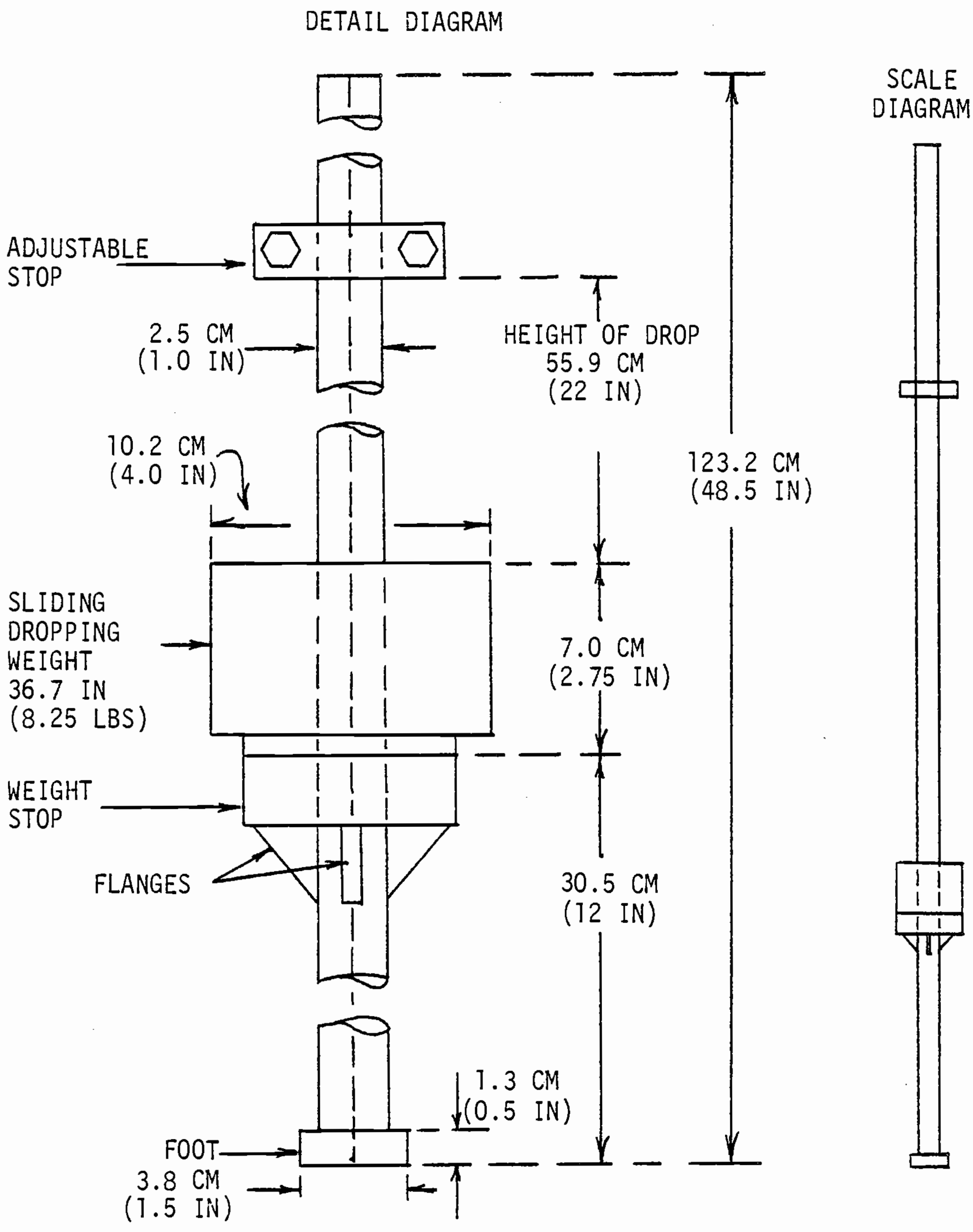

Figure 3. Gus Probe.

constant distance. The weight impacts a flat plate, transferring the energy acquired from the drop to the plate and to a foot which is driven into the soil. Factors affecting penetration of the foot into the soil could describe soil resistence to compaction.

The tool, called the Gus Probe, was designed to withstand harsh treatment, to be relatively easy to use after minimal training, and to transfer constant energy levels to the foot for each drop of the hammer. The foot of the Gus probe is positioned vertically on a selected point and kept in this location and position until the completion of the test. A diagram of the Gus Probe is given in Figure 3.

The Gus samples were taken in the same 0.91 by 0.91 meter square as the cone penetrometer readings or adjacent to the penetrometer readings outside the test strip if insufficient time was available to take them inside the test strip prior to commencing skidding. Several different types of readings were taken with the Gus probe to allow us to determine which would be the most useful indicator of the soil's response to logging equipment impacts. The measurements of penetration per drop for a total of 20 drops were used to generate five independent variables. The five independent variables are discussed further in the Gus Probe Analysis section of this paper. Ten samples for each strip measured total penetration following 20 drops. Ten samples for each strip measured the number of drops required to pass the 10.2 cm (4 in.) depth. Five of the ten measurements of total penetration and five of the ten measurements of number of drops required to pass the 10.2

cm depth were made while recording penetration per blow.

Site preparation for use of the Gus probe was accomplished by carefully removing the litter layer to expose the mineral soil immediately below the fungal mycelia. A stake was securely pounded into the ground very close to the position of the probe. The probe was gently lowered vertically to rest the foot of the probe on the exposed soil. Later in the testing, the stake was replaced by a tripod which also served to support the probe in the vertical position. An initial reading of the vertical distance between a reference mark on the hammer and the top of the stake was recorded. Subsequent readings were taken from the reference mark to the top of the stake and penetration of the foot recorded as the difference from the initial reading. Care was taken to keep the hammer plumb during testing; however, the awkward posture required to operate the hammer made that difficult. A level was used to facilitate plumbing the hammer prior to taking the penetration readings. Some inaccuracies were introduced by unavoidably rocking the hammer while testing, failure to keep the hammer perfectly plumb while making the sinkage readings in spite of the use of the level, and increasing error with sinkage as the angle between the reference mark on the hammer and the top of the stake increased.

GUS PROBE ANALYSIS

The purpose of the Gus probe readings was to determine an average soil response for each skid trail to the hammer blows prior to any equipment travel. It was hypothesized that measurements of the behavior of the Gus probe could be used to predict soil compaction resulting from the use of the logging vehicles.

Ten Gus probe measurements were taken for each test strip within the 14.63 meter by 3.66 meter (48 feet by 12 feet) test plot at points randomly located in reference to the sixty-four 0.91 meter by 0.91 meter (3 feet by 3 feet) square grid elements created for the density probe. The Gus probe squares were selected to ensure that they would not coincide with a density probe square because the impact of the Gus probe would affect the density measurements. If insufficient time was available prior to commencing the skidding operations to permit sampling within the test plot, the Gus samples were taken at randomly located points immediately outside. Ten measurements, described earlier, were averaged for each strip. The Gus probe was unable to penetrate the excessively rocky soil on three test plots on the Pliocene Ridge site. No data were included in the regression analysis for these plots. Five potentially significant parameters were identified to describe the behavior of the Gus probe, as follows:

GUSB4 is the number of blows, or drops of the weight, required to drive the bottom of the foot of the probe 10.2 cm

(4 inches), below the surface of exposed mineral soil.

GUSTP quantifies the total penetration, in centimeters, of the bottom of the foot of the probe resulting from 20 drops of the weight.

GUSS1 measures the slope of the initial straightline segment of the penetration per blow plot, as shown in Figure 3, expressed in centimeters per blow.

GUSS2 measures the slope of the final straightline segment of the penetration per blow plot, as shown in Figure 4, expressed in centimeters per blow.

GUSSB is the depth of the break in slope between the initial and final straightline segments of the penetration per blow plot, measured in centimeters.

The dependent variable in the predictive equation was to be a measure of compaction resulting from the use of the three ground-based logging vehicles. As discussed in the Literature Review, compaction resulting from the use of ground-based logging vehicles seldom extends below 30.5 cm (12 in.), with the greatest compaction taking place in the upper 20 cm (7.9 in.) where most of the small roots of trees are located. At all sites the stoniness of the soils tested increased with depth. For these reasons, only the surface 20.3 cm (8 in.) were used in the predictive model for the dependent variable. Further, understanding the compaction in the surface layers should lead to an understanding of the compaction occurring in the lower layers.

CD08 is the average change in density for the surface 20.3 cm (8 in.) expressed in grams per cubic centimeter, resulting from 20 trips of the logging vehicles.

No attempt was made to separate the effects of the different machines on ultimate change in density, nor was an attempt made to evaluate compaction resulting from fewer than 20 trips.

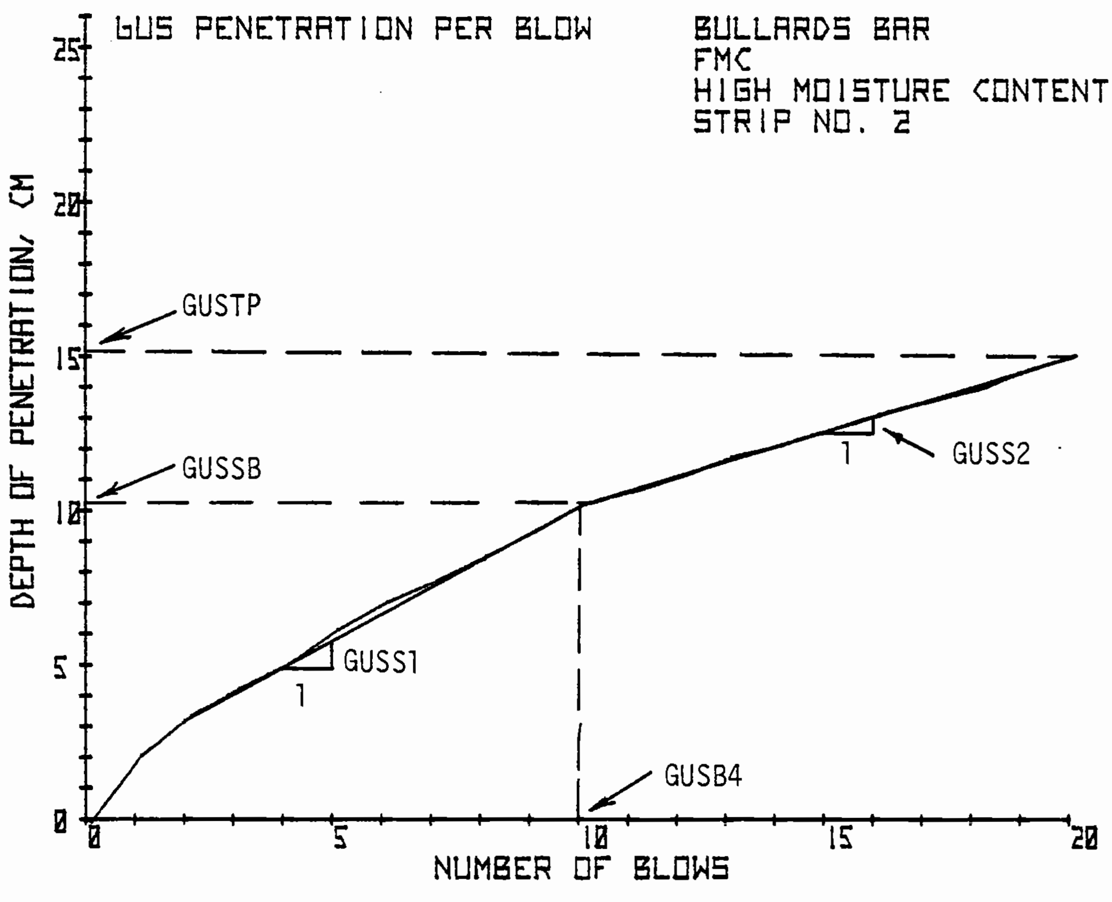

Figure 4. Diagram of Gus Probe Independent Variables, One Example.

The Gus probe was developed to serve as an easy to use, indestructable predictive tool for estimating compaction resulting from the use of ground-based logging vehicles. The regression equation for predicting compaction was kept simple. Easy to measure variables and simple regression calculations were emphasized, assuming the parameters and the regression proved to be statistically significant. Simplicity, within the bounds of statistical significance, was stressed.

Occasionally, the 10.2 cm (4 in.) depth could not be attained with reasonable effort due to roots, rocks or hard soil. When the probe was unable to pass the 10.2 cm (4 in.) depth, the maximum number of blows recorded for a successful penetration, 80 blows, was entered as the value of GUSB4 for the observation.

An additional independent variable reflecting the average soil moisture content to the 30.5 cm (12 in.) depth was added to the regression analysis.

MC is the average moisture content, expressed in percent, of the ten moisture content samples obtained near the density probe plots.

Gus Probe Regression Analysis

The regression analysis was performed using the Stepwise and Backstep routines with the SIPS statistical package. The risk of encountering a Type I error was set at .05. Although statistically significant predictive equations are given for each site and for all sites combined, this author does not recommend the use of the equations without further validation. A discussion of the equations follows the presentation of the equations. In the regression equations which follow:

CD08 = change in soil density, in g/cc, to the 20.3 cm (8 in.) depth following 20 trips of the logging vehicles.

GUSB4 = number of blows required to pass the 10.2 cm (4 in.) depth.

GUSTP = total penetration of the probe, in centimeters.

GUSS1 = slope of the initial straightline segment of the penetration per blow plots.

GUSS2 = slope of the final straightline segment of the penetration per blow plots.

GUSSB = depth, in centimeters, of the break in slope between the straightline segments of the penetration per blow plots.

MC = average soil moisture content to the 30.5 cm (12 in.) depth, in percent.

n = number of observations.

* = indicates the regression coefficient associated with the variable is significantly different from zero at the .05 probability level.

** = indicates the regression coefficient associated with the variable is significantly different from zero at the .01 probability level.

*** = indicates the regression coefficient associated with the variable is significantly different from zero at the .001 probability level.

MOONSHINE

$$CD08 = 0.2622 - 0.002887(GUSB4)^{**} - 0.01328(GUSSB)^{*}$$

$n = 9$, $R^2 = .7096$

Expressed in U.S. Customary Units ($lbs.-ft.^{-3}$):

Density Change = 16.36
-0.1802(GUSB4,blows)
-0.8288(GUSSB,inches)

BULLARDS BAR

$$CD08 = .04241 - 0.5844(GUSB4)^{**} - 0.3069(GUSS1)^{***}$$

$n = 9$, $R^2 = .8389$

Expressed in U.S. Customary Units ($lbs.-ft.^{-3}$):

Density Change = 26.47
-0.3649(GUSB4,inches)
-19.15(GUSS1,inches per blow)

PLIOCENE RIDGE

$$CD08 = 0.3863 - 0.4125(GUSS2)^{***} - 0.003338(MC)^{***}$$

$n = 6$, $R^2 = .9953$

Expressed in U.S. Customary Units ($lbs.-ft.^{-3}$):

Density Change = 24.11
-25.75(GUSS2,inches per blow)
-0.2084(MC,percent)

YUBA PASS

$$CD08 = -0.001366 \qquad n = 9$$

$$+0.1986(GUSS1)^{*} \qquad R^2 = .6004$$

Expressed in U.S. Customary Units (lbs.-ft.$^{-3}$):

Density Change = -0.08522

+12.39(GUSS1,inches per blow)

ALL SITES COMBINED

$$CD08 = 0.2070 \qquad n = 33$$

$$-0.002239(GUSB4)^{***} \qquad R^2 = .5730$$

$$-0.002728(MC)^{***}$$

Expressed in U.S. Customary Units (lbs.-ft.$^{-3}$):

Density Change = 12.92

-0.1398(GUSB4,blows)

-17.03(MC,percent)

The high coefficients of determination for the site specific regression equations are the result of a relatively large number of variables in a model with few observations. A check of the significant variables by site and in total shows that the predictor variables required for any one site are not significant for any other site. This suggests detailed soils information is required before a determination can be made concerning which site specific predictive equation is applicable. The regression equation for all sites combined would not give meaningful estimates of compaction because on no specific site were the variables GUSB4 and MC statistically significant. The regression equations are included in this paper because this author feels further work is warranted on a tool of similar design philosophy. The equations may help facilitate further work. A further discussion of potentially significant Gus parameters for further work is contained in this paper in the Comparison of the Gus Probe and the Cone Penetrometer sections. Because use of the predictive models is not recommended, further discussion is not warranted.

Modification of the design of the Gus probe recommended by operators include adding a level bubble to facilitate plumbing the tool, mounting a handle on the dropping weight, supporting the tool vertically with an adjustable tripod, and permitting the tool to be broken down into its component parts to facilitate transport. The long rod could be made of aluminum or hollow steel plumbing pipe to lighten the tool. A scale could be scribed on the shaft of the tool to facilitate making penetration measurements. Additional design considerations are given in the comparison with the cone penetrometer.

CONE PENETROMETER ANALYSIS

Ten cone penetrometer measurements were taken for each of the 36 test strips. The measurements were taken inside the 48-foot test plot within the same 0.91 meter by 0.91 meter (3 ft by 3 ft) square grid elements used for the Gus probe sample. The size of the grid was large enough so that both samples could be taken without interference. If insufficient time was available to obtain the sample within the test plot prior to commencing skidding operations, the sample was obtained from randomly located points immediately outside of the test strip.

Penetrometer dial readings were recorded for penetrations of 10.2 cm and 15.2 cm (4 and 6 in.) of the penetrometer cone tip. The recorded dial readings correspond to penetrations of 5.1 and 10.2 cm (2 and 4 in.) respectively, of the penetrometer cone shoulders. A 30 degree, 5.1 cm (2 in.) high cone was used throughout the testing. The penetrometer dial readings were converted to cone indices according to the regression equation developed in Appendix A.

If the person operating the cone penetrometer was unable to penetrate the soil to the desired depth, a note to that effect was entered in the field data sheet in lieu of a dial reading for the depth being measured. The maximum dial reading for a successful penetration, 1128, was used as the dial reading for all points in which the operator was unable to penetrate the soil to the desired depth. The cone index was calculated for these points using the standard regression equation developed in Appendix A. Roots, rocks and hard soil prevented penetration as observed with the Gus probe. Hard soil was encountered on the Moonshine site with low moisture content samples.

The cone penetrometer was examined for use as a predictive tool for estimating soil compaction resulting from the use of the three ground-based logging vehicles because penetrometers are readily, commercially available, easy to use, and are familiar to a large number of people.

The average cone index from the ten samples taken for each strip evaluated by site and in total, to develop a statistically significant equation for predicting compaction. Soil compaction was defined as the change in soil density, expressed in grams per cubic centimeter, of the soil following 20 trips of the three logging vehicles. As defined for the Gus probe, only the average change in density to the eight inch layer was examined for each strip. No attempt was made to separate the effects of the three machines individually. Moisture content, as defined for the Gus probe analysis, was included in the regression analysis. The regression analysis indicated low significance for the cone index readings to the 10.2 cm (4 in.) depth. In the opinion of this author, the 10.2 cm readings lacked consistency and reflected the effect of surface organic matter and not the effects of soil strength, even though the penetration measurements were started below the fungal mycelia layer. The cone penetrometer was designed to estimate trafficability of soils by obtaining an estimate of soil strength. For these reasons, the 10.2 cm readings were not considered in the regression analysis.

Regression analysis was performed using the Stepwise and Backstep routines contained within the SIPS statistical package. The risk of encountering a Type I error was set at .05. In the regression equations which follow:

CD08 = the change in soil density, in g/cc, resulting from 20 trips of the logging vehicles, averaged to the 20.3 cm (8 in.) layer for each strip; the dependent variable.

CI6 = the average cone index, in psi, required to push the cone tip to the 15.2 cm (6 in.) depth for each strip.

MC = the average soil moisture content for each strip to the 30.5 cm (12 in.) depth, in percent.

n = number of observations.

** = indicates the regression coefficient associated with the variable is significantly different from zero at the .01 probability level.

*** = indicates the regression coefficient associated with the variable is significantly different from zero at the .001 probability level.

<u>MOONSHINE</u>

CD08 = 0.2900 $\quad$ n = 8

-0.0007802(CI6)** $\quad$ R^2 = .7866

TABLE III. ANOVA OF CI6 AND CD08, MOONSHINE.

SOURCE	DF	SUM OF SQUARES	MEAN SQUARE
TOTAL	8	0.0189489	0.0023681
REGRESSION	1	0.0131092	0.0131092
RESIDUAL	7	0.0058397	0.0008342

Expressed entirely in SI units:

CD08 = 0.2890

-0.0001132(CI6,in kPa)

Expressed entirely in U.S. Customary Units (lbs-ft^{-3})

Density change = 18.10

-0.04871(CI6,in psi)

BULLARDS BAR

CD08 - 0.2531 $n = 9$

-0.0006828(CI6)** $R^2 = .6918$

TABLE IV. ANOVA OF CI6 AND CD08, BULLARDS BAR.

SOURCE	BF	SUM OF SQUARES	MEAN SQUARE
TOTAL	8	0.0189489	0.0023686
REGRESSION	1	0.0131092	0.0131092
RESIDUAL	7	0.0058397	0.0008342

Expressed entirely in SI units:

CD08 = 0.2531

-0.00009904(CI6,in kPa)

Expressed entirely in U.S. Customary Units (lbs-ft^{-3}):

Density Change = 15.80

-0.04263(CI6,in psi)

PLIOCENE RIDGE

CD08 = 0.2867 $\quad$ n = 9

-0.0008350(CI6)*** $\quad$ R^2 = .9011

TABLE V. ANOVA OF CI6 AND CD08, PLIOCENE RIDGE.

SOURCE	DF	SUM OF SQUARES	MEAN SQUARE
TOTAL	8	0.0143880	0.0017985
REGRESSION	1	0.0129645	0.0129645
RESIDUAL	7	0.0014235	0.0002034

Expressed entirely in SI units:

CD08 = 0.2867

-0.0001211(CI6,in kPa)

Expressed entirely in U.S. Customary Units (lbs-ft^{-3}):

Density Change = 17.90

-0.05213(CI6,in psi)

YUBA PASS

A statistically significant regression equation for predicting compaction using the variables CI6 and MC could not be generated while controlling the probability of incurring a Type I error at .05. Allowing a slackening of the probability results in the following equation, significant at the .17 probability level.

CD08 = 0.2283 $\qquad$ n = 9

-0.0004844(CI6) $\qquad$ R^2 = .2608

TABLE VI. ANOVA OF CI6 AND CD08, YUBA PASS.

SOURCE	DF	SUM OF SQUARES	MEAN SQUARE
TOTAL	8	0.0107740	0.0013467
REGRESSION	1	0.0028094	0.0028094
RESIDUAL	7	0.0079646	0.0011378

Expressed entirely in SI units:

CD08 = 0.2283

-0.00007025(CI6,in kPa)

Expressed entirely in U.S. Customary Units (lbs-ft^{-3}):

Density Change = 14.26

-0.0302(CI6,in psi)

ALL SITES COMBINED

$$CD08 = 0.2631 - 0.0007044(CI6)^{***} \qquad n = 35 \qquad R^2 = .7339$$

TABLE VII. ANOVA OF CI6 AND CD08, ALL SITES COMBINED.

SOURCE	DF	SUM OF SQUARES	MEAN SQUARE
TOTAL	34	0.0749287	0.0022038
REGRESSION	1	0.0549913	0.0549913
RESIDUAL	33	0.0199374	0.0006042

Expressed entirely in SI units:

$$CD08 = 0.2631 - 0.0001022(CI6,\text{in kPa})$$

Expressed entirely in U.S. Customary Units ($lbs\text{-}ft^{-3}$):

$$\text{Density Change} = 16.42 - 0.04643(CI6,\text{in psi})$$

None of the equations found moisture content to be a statistically significant variable throughout the ranges of moisture content encountered in the tests. A statistically significant regression equation could be generated for Yuba Pass using the cone index readings for the 10.2 cm (4 in.) depth, but this author does not feel the introduction of an additional variable would improve the usefulness of the predictive models. The high coefficients of determination for all sites except Yuba Pass indicate the cone penetrometer can be used for predicting compaction. Plots of the data indicate a linear relationship between CD08 and CI6. Because no obvious trend is evident in comparing the soil plasticity with either the regression constants or slopes, this author recommends using the regression equation for all sites combined in any attempts to validate the models unless very similar soils are encountered. A validation phase is an obvious requirement prior to the acceptance of any of the models.

It is important to remember that the regression equations pertain to averages of ten cone index and ten density measurements for each strip. Only the averages were regressed by site and in total. Averaging the data in this manner would have the effect of masking the occasionally high variability of the cone index measurements.

The equations also pertain only to areas which are in well-defined skid trails subjected to the impacts of 20 round trips of the logging vehicles used in this study. The regression equations should not be expected to be valid throughout a logging unit in which some areas would remain undisturbed and some areas would be impacted with more than 20 trips of the logging vehicle.

Penetration to the 15.2 cm depth was more frequently not possible on the Moonshine and Pliocene Ridge sites than on the other two sites. The Pliocene Ridge site contained numerous large rocks which precluded penetration. The soil on the Moonshine site became very hard at low moisture contents. A relatively high value for dial reading was used for samples in which the cone tip could not be pushed to the 15.2 cm depth. The effect of frequent unsuccessful penetrations would be to create a higher average cone index for a strip than would be indicated by soil strength alone. The Moonshine site soil was stronger at lower moisture contents and the assumed high cone index value accurately reflects this property. The unsuccessful penetrations on Pliocene Ridge, however, resulted from rocks and did not reflect soil strength properties. The unsuccessful penetrations would have the effect of falsely indicating high soil strength. The rocks may have been in contact with one another and acted to absorb the impacts of the logging vehicles, thus reducing soil compaction. The effect of the rocks on Pliocene Ridge would be to cause high cone index readings to be associated with low levels of soil compaction. This effect is reflected in the high coefficient of determinations for the regression equation.

Unsuccessful penetrations on Yuba Pass, the other cohesionless soil tested, were the result of roots in the soil. The effect of the roots would be to raise the cone index readings, yet the soil may have been compacted significantly. The small and flexible roots would not absorb the impacts of the vehicles as efficiently as the rocks on Pliocene Ridge. The low coefficient of determination for the Yuba Pass regression equation may possibly be explained by this argument. Only rarely were roots encountered at the 10.2 cm (4 in.) penetration depth. A statistically significant regression equation was derived for the cone index values at the 10.2 cm depth, indicating the cone index values are accurate predictors of soil compaction if the effect of roots can be eliminated. The cone penetrometer appears to warrant further work to validate the models. If an unsuccessful penetration occurs, the reason for the unsuccessful penetration should be determined. If rocks or hard soil caused the unsuccessful penetration, the sample should be retained and the plastic deformation loading of the proving ring used for an indicated dial reading. If roots caused the unsuccessful penetration, additional samples should be taken until either a successful penetration is achieved or rocks or hard soil are encountered.

COMPARISON OF THE GUS PROBE AND THE CONE PENETROMETER

Based upon the statistical analyses for the Gus probe and the cone penetrometer, both tools appear to be useful for predicting soil compaction. However, the penetrometer regressions are more useful because the statistically significant independent variable remains constant between sites. The Gus probe is inconsistent. Detailed soils information is required to determine which regression equation to use to predict compaction. The need for detailed soil information violates the intention of designing an easy to use predictive tool.

The Gus tool was designed to be an easy-to-use predictive tool for soil compaction, but the regression analysis lacked consistency. A statistical comparison between the Gus variables and the cone indices to aid in redesign of the tool is in order. The statistical analysis was performed using the Stepwise and Backstep routines contained within the SIPS statistical package. The risk of a Type I error was controlled at the .05 probability level. Only the significant variables are listed without their coefficients or the dependent variable axis intercept. In the regression equations which follow:

CI6 = the cone index, in psi, required to push the cone tip to the 15.2 cm (6 in.) depth.

GUSB4 = the number of blows required to pass the 10.2 cm (4 in.) depth.

GUSS1 = the slope of the initial straightline segment of the penetration per blow plots.

GUSS2 = the slope of the final straightline segment of the penetration per blow plots.

GUSSB = the depth, in centimeters, of the break in slope between the strightline segments of the penetration per blow plots.

f = is a function of:

Moonshine:	CI6 = f(GUSB4,GUSSB)
Bullards Bar:	CI6 = f(GUSB4)
Pliocene Ridge:	CI6 = f(GUSSB,GUSS2)
Yuba Pass:	CI6 = f(GUSS1)
All Sites Combined:	CI6 = f(GUSB4)

Statistically significant Gus variables can predict cone indices, a recognized measure of soil strength and a potential predictor of soil compaction. The predictor variables for estimating cone indices tend to be the same predictor variables for soil compaction. This suggests that further work with a tool similar to the Gus probe is warranted if the durability concept of the Gus probe is to be achieved. A redesign of the Gus probe may help to bring one variable into focus as a significant predictor and thus eliminate the need for detailed soils information. The following points are the result of observing the behavior of the probe on the four sites at different moisture contents and reflect the opinion of the author.

1. The soil shock loading resulting from the dropping weight appeared to be excessive. Either the height of drop should be reduced, which would facilitate use of the tool, or the weight could be reduced, or both. Reducing the magnitude of the shock loading would have the effect of refining the accuracy of the measurements. Taken to the extreme, a great reduction in shock loading would simulate compactive loadings rather than bearing capacity failures with the rapid mobilization of shear failure surfaces, but data collection without a mechanized tool would be an onerous endeavor.
2. Various foot sizes could be tried. In order to reduce the pressure loading on the foot one could increase the diameter of the foot; however, the probability of having to abort a sample because the probe was unable to penetrate to a desired depth due to encountering roots, rocks or hard soil would be increased. Reducing the impact loading by reducing the dropping weight or reducing the distance through which the weight drops would be preferable if roots or rocks are likely to be encountered. Using standard cone penetrometer tips on a dropping hammer tool is also suggested.
3. Design modifications would make the tool easier to use. Suggested modifications include providing a stable tripod support to keep the tool plumb while being operated, adding a level bubble, adding a handle on the weight to facilitate

lifting, scribing a scale on the shaft of the tool to permit direct penetration readings, and allowing the tool to be disassembled.

In the opinion of this author, the potential is high for development of a durable and easy to use tool based on the concept of the Gus probe.

SOIL COMPACTION BY MACHINE TYPE

The bulk density versus depth relationships shown in Figures 5, 7, 9, and 11 depict the initial average soil densities for all nine strips for each site and the final densities after 20 trips by each machine. The final densities are averages across all moisture classes from the three strips for each machine at each site.

The undisturbed soil density curves show the usual increase in soil density with depth as a result of consolidation. The curves show definite changes in the rate of consolidation with depth, a result of connecting discrete data points with straight lines. The density increase would be more accurately depicted by smooth curves connecting the data points. The indicated density decrease between the 15.2 cm and 20.3 cm (6 and 8 in.) depths in Figure 5 probably represents a layer of root accumulations from the original dense brush undergrowth. An anomaly in the data can be ruled out because all plots of densities following skidding show the same effect. An anomaly in the data would not be repeated consistently.

The diagrams illustrating density increases by machine in Figures 6, 8, 10, and 12 show the increases in soil density for all measured depths for each machine averaged for each site. For each site, the densities of undisturbed soil were averaged for each machine for each depth, then the ultimate densities were averaged for each machine for each depth. Figures 6, 8, 10, and 12 show the differences, expressed in grams per cubic centimeter, between the undisturbed and ultimate densities.

The Moonshine site is a low elevation site with a dense, slightly plastic, sandy loam soil. As shown in Figure 5, the FMC attained the highest ultimate density at the 5 centimeter (2 in.) depth and at the 30.5 centimeter depth (12 in.), but the machines were essentially comparable through the range of intermediate depths. The magnitude of the differences in densities even at the 5 centimeter and 30.5 centimeter depths are not great. All machines caused comparable ultimate densities.

The increase in soil density on the Moonshine site (Figure 6) shows little difference between machines at the five centimeter depth. The tractor caused larger density increases at greater depths. Little compaction is shown for both the skidder and the FMC at depths greater than 10.2 centimeters (4 in.). The tractor curve shows the soil is still being compacted at the 30.5 centimeter depth. The tractor change in bulk density with depth at Moonshine (Figure 6) is greater than the changes observed for the other machines. The absolute density curves (Figure 5) show all three machines attaining comparable absolute densities. The reason the tractor curve shows a larger density change to attain comparable absolute density is that the soil was less dense initially. As shown in Figure 6, the FMC caused less soil compaction at depths greater than five centimeters on this slightly cohesive, dense soil.

The Bullards Bar site exhibits a slightly plastic, loose, loam

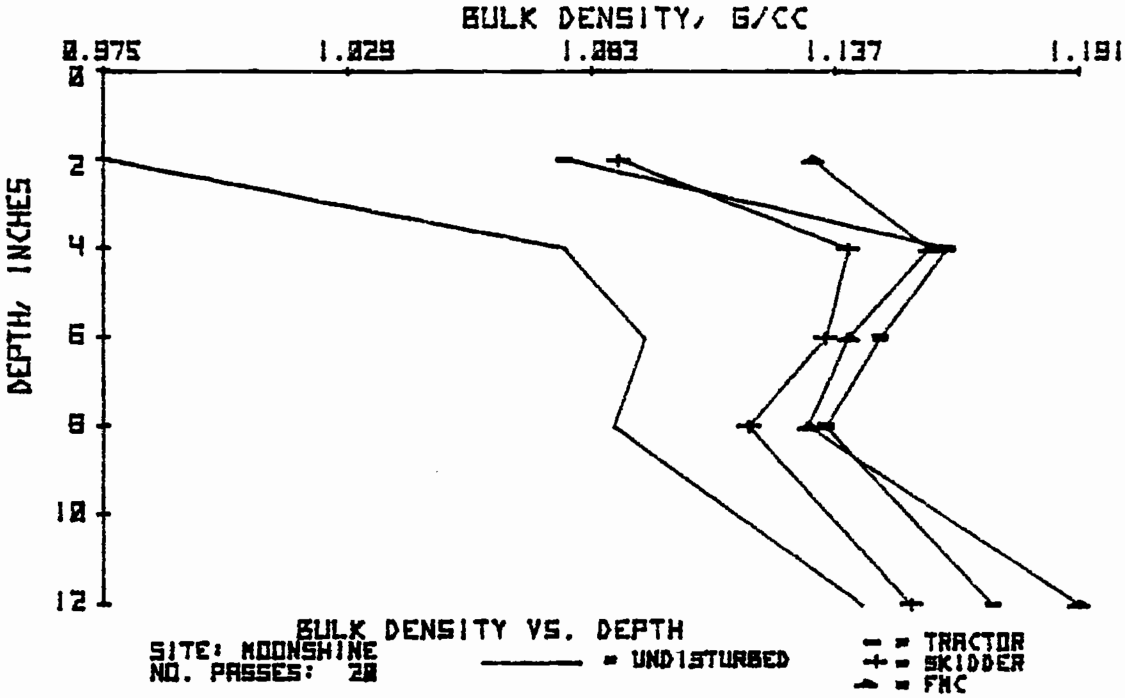

Figure 5. Moonshine Bulk Densities Before and After Skidding. The solid line is the average density of all nine strips.

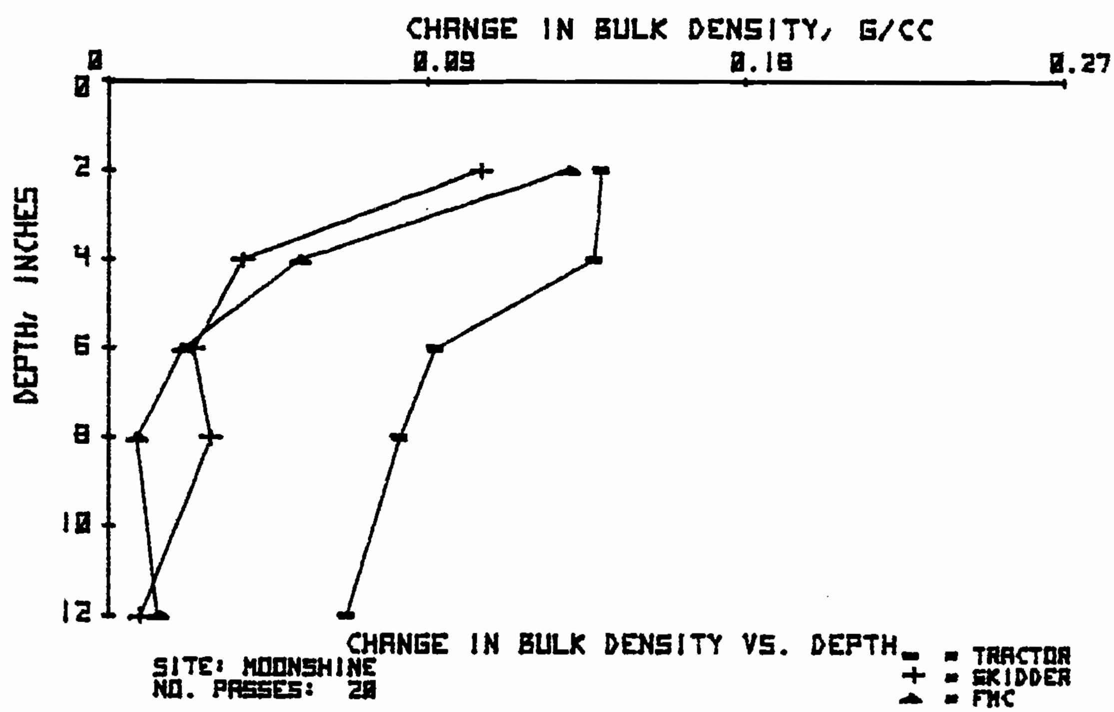

Figure 6. Moonshine Density Increase by Machine.

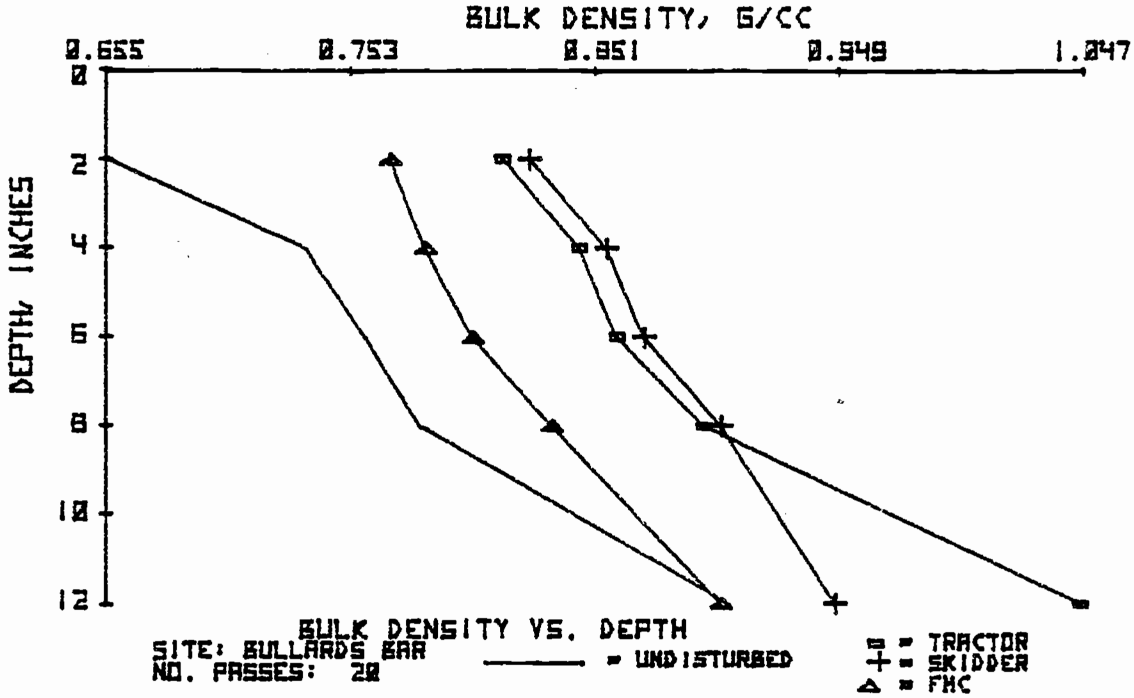

Figure 7. Bullards Bar Densities Before and After Skidding. The solid line is the average density of all nine strips.

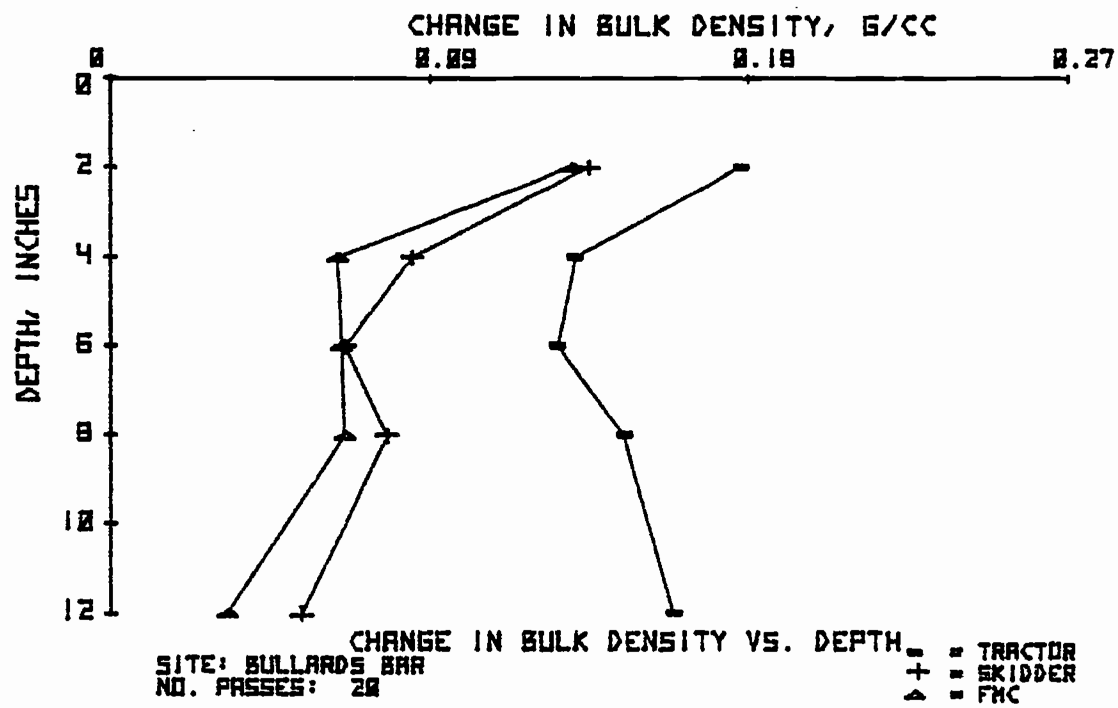

Figure 8. Bullards Bar Density Increase by Machine.

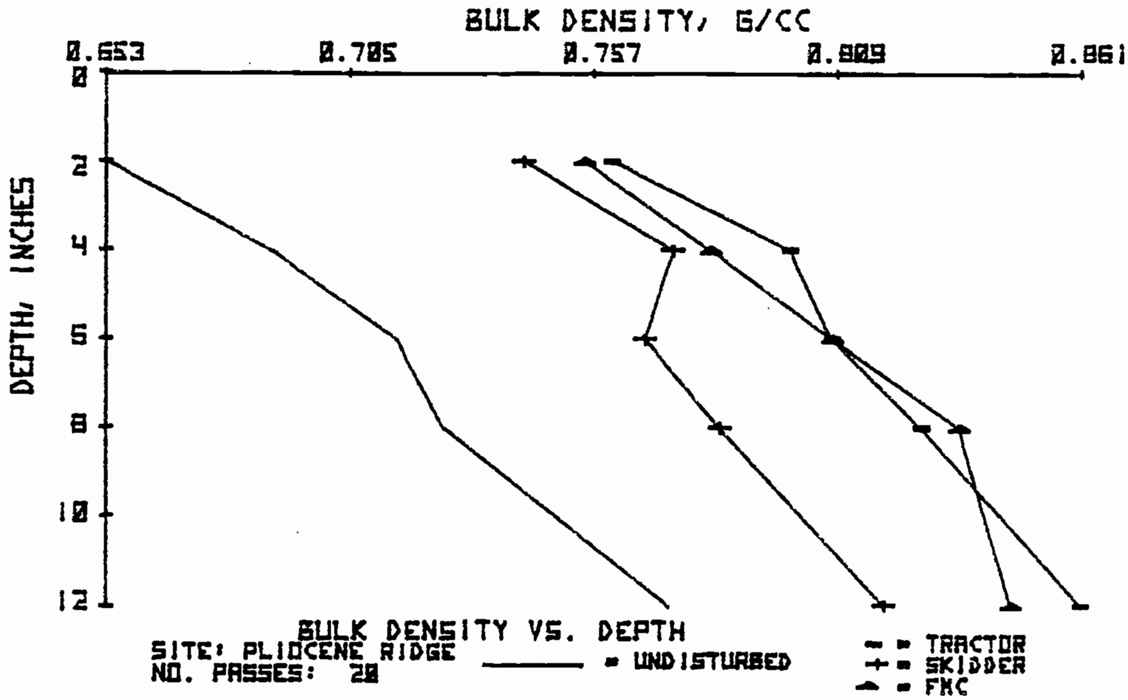

Figure 9. Pliocene Ridge Densities Before and After Skidding. The solid line is the average of all nine strips.

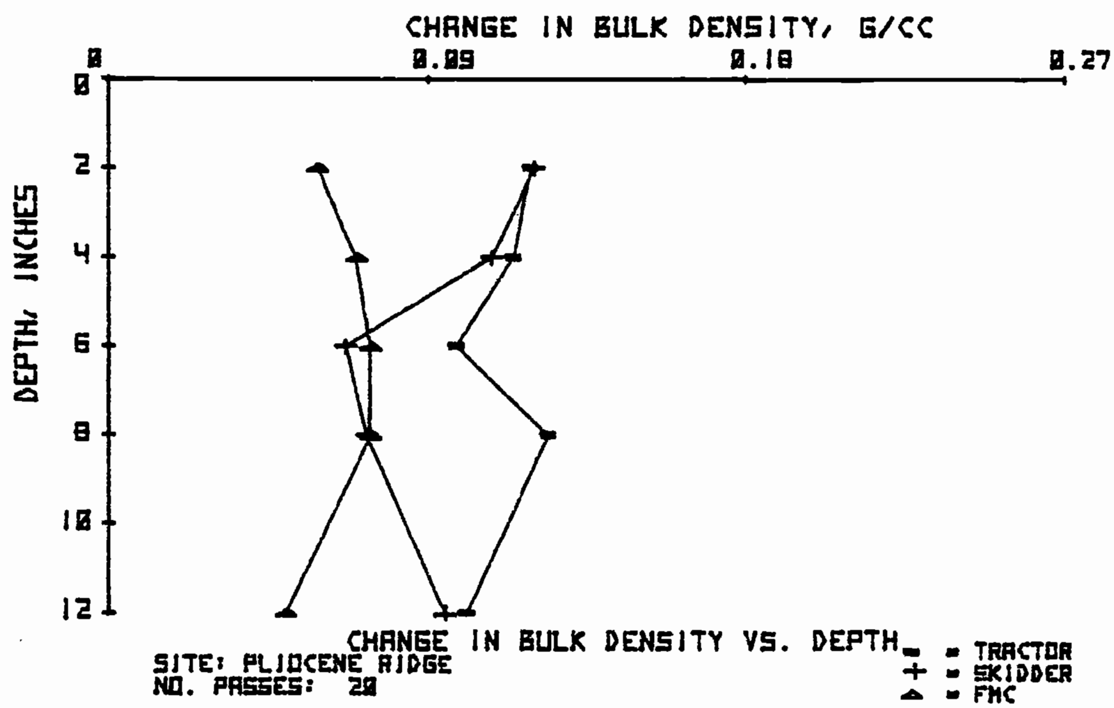

Figure 10. Pliocene Ridge Density Increase by Machine.

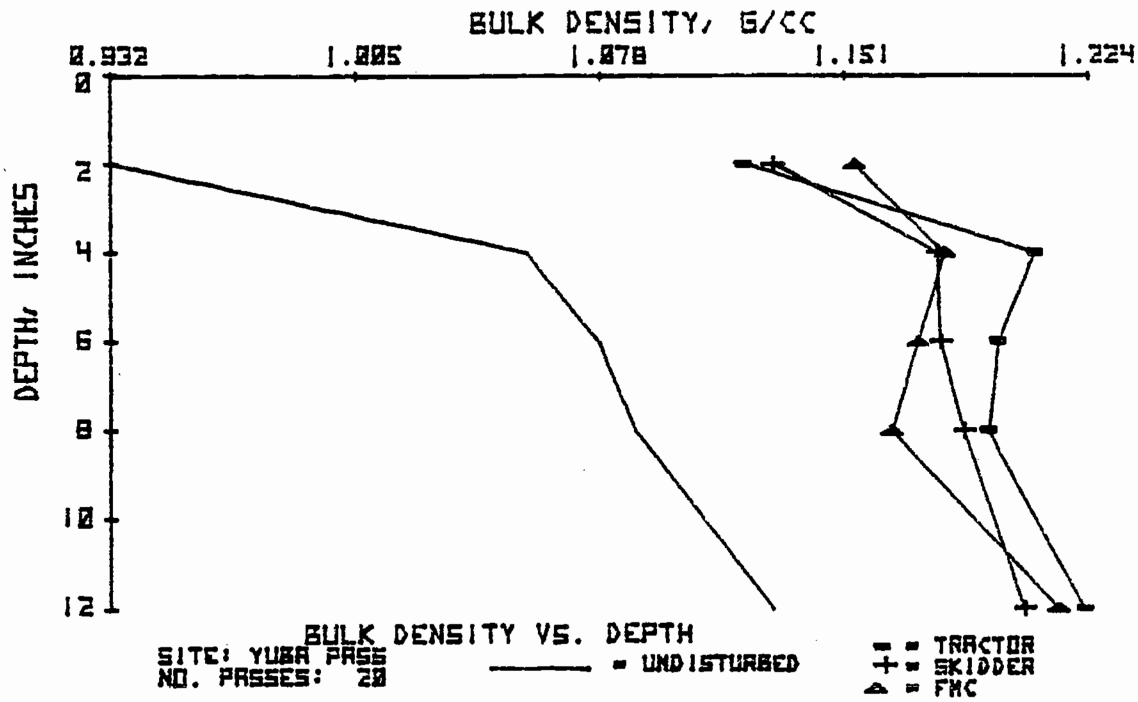

Figure 11. Yuba Pass Densities Before and After Skidding. The solid line is the average density of all nine strips.

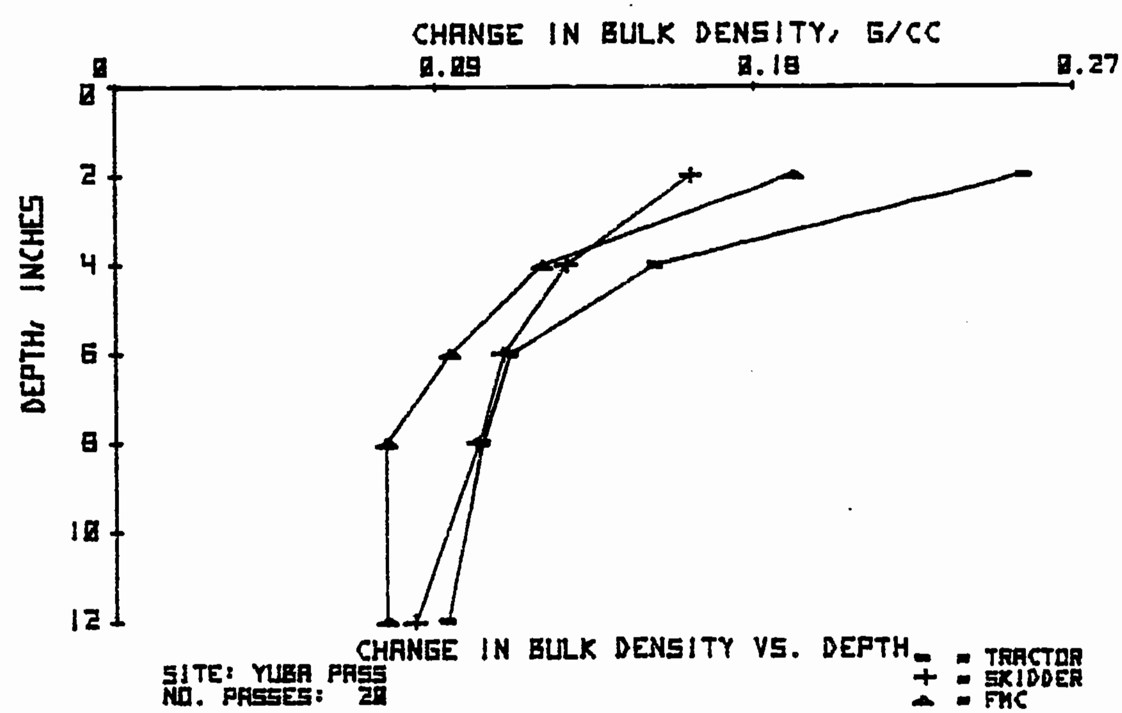

Figure 12. Yuba Pass Density Increase by Machine.

soil. Figure 7 shows a definite difference in machines at the 30.5 centimeter (12 in.) depth with the tractor causing the greatest ultimate density and the FMC the least. The FMC caused the least ultimate density at all depths. The densities attained by the tractor and the skidders are essentially identical at depths less than 30.5 centimeters. The density increases caused by the skidder and the FMC, shown in Figure 8, are very comparable. They are less than the density increases caused by the tractor at all depths. Again, these results are not reflected in the curves of the absolute densities (Figure 7), which show the FMC to be markedly different from the skidder to the 20.3 centimeter (8 in.) depth. In Figure 5, the skidder differs from the tractor only at the 30.5 centimeter depth. The increase in compaction indicated for the tractor curve in Figure 8 from the 20.3 centimeter (8 in.) depth to the 30.5 centimeter depth probably is not an accurate portrayal of the actual density increases. Data points were lost because the probe could not consistently be pushed to the 30.5 centimeter depth. The density curves for the 30.5 centimeter depth reflect the data from the points which could be successfully maintained throughout the test.

Greater deep compaction occurred at the Bullards Bar site than at the Moonshine site. Given a loose, slightly cohesive soil, the skidder and the FMC cause comparable soil compaction at all measured depths. The tractor caused the most compaction at all depths.

The Pliocene Ridge site has a non-plastic, loose, loamy sand soil with a high percentage of coarse fragments. Increases in soil density (Figure 10) are less at the five centimeter (2 in.) depth for the FMC than the skidder or tractor. The differences between machines at greater depths are inconclusive. The absolute soil densities (Figure 9) at five centimeters reflect the effects of initial densities and not the changes resulting from the skidding operations. The differences between the absolute density and the change in density are most clearly shown in the skidder data. The skidder strips were initially less dense than the tractor or FMC strips. The data is again incomplete for the 30.5 centimeter depth for the tractor and skidder curves. Therefore, the indicated increase in compaction between the 20.3 centimeter (8 in.) depth and the 30.5 centimeter depth on the skidder curve is probably not an actuality.

Given a loose, non-plastic soil, the FMC caused less compaction than the tractor or the skidder at the five centimeter depth, but the machines caused roughly comparable levels of compaction at greater depths.

The Yuba Pass site was the site at the highest elevation. The soil was a dense, non-plastic, loamy sand. As was shown previously for the other dense soil at the Moonshine site, little difference in ultimate densities is in evidence between machines (Figure 11). The lack of identifiable differences between machines is even more pronounced on the cohesionless Yuba Pass site. The tractor (Figure 12) caused the greatest increase in soil density observed for any machine on any site. This occurred at the five centimeter (2 in.) depth. All machines caused comparable density increases at depths greater than five centimeters. The slopes of the density increase graphs indicate little reduction in compaction between the 20.3 centimeter (8 in.) depth and the 30.5 centimeter (12 in.) depth.

Dense, non-plastic soils, as represented by the soil at Yuba Pass, seem to be compacted comparably at depths greater than five centimeters by all three machines. The skidder, perhaps reflecting the kneading compactive effort of the rubber tires, compacted the surface five centimeters the least, with slightly greater compaction resulting from the FMC.

Differences discussed in absolute density and the change in density point out the importance of focusing on the change in densities encountered before and after skidding. All four test sites were carefully selected to ensure freedom from prior disturbances which could have compacted the soil in any way, yet the densities attained after 20 trips for all three vehicles on the Pliocene Ridge site, as shown in Figure 9, were less than the undisturbed densities on the Moonshine and Yuba Pass sites, as shown in Figures 5 and 11. Lull (1959) notes that compaction is best measured as a change in density.

The slightly cohesive soils show less soil compaction for the skidder and FMC than the cohesionless soils at the 30.5 centimeter depth. Compaction caused by the tractor is evident even at the 30.5 centimeter depth for all soils.

SOIL DISTURBANCE

The soil disturbance profiles are presented in Appendix C of this paper. Soil disturbance in this paper is defined as the change in elevation of the mineral soil surface before skidding and following 20 round trips. Soil disturbance includes the effects of soil displacement, as well as soil compaction.

Hubs of equal elevation were located on either side of the 14.63 meters (48 feet) by 3.66 meters (12 feet) test plot perpendicular to the orientation of the test strip. A tape was stretched tightly between the hubs and the distance from the tape to the mineral soil surface was recorded for all obvious terrain breaks across the strip. The area between the tightly stretched tape and the soil surface was calculated before and after skidding; the area disturbed was calculated as the difference between the two areas. The relative soil disturbances are plotted in Figure 13. All trails were carefully controlled in alignment, moisture content, entrance and exit, and were in close proximity to each other. The crawler tractor and the FMC were skidding the same turn weights and, therefore, are directly comparable. The average wheeled skidder turn weight was only 54 percent of the average tractor/FMC turn weight.

A careful examination of the profile plots in Appendix C shows soil accumulations in the center of the trail as well as at the edges of some of the trails. The soil accumulation in

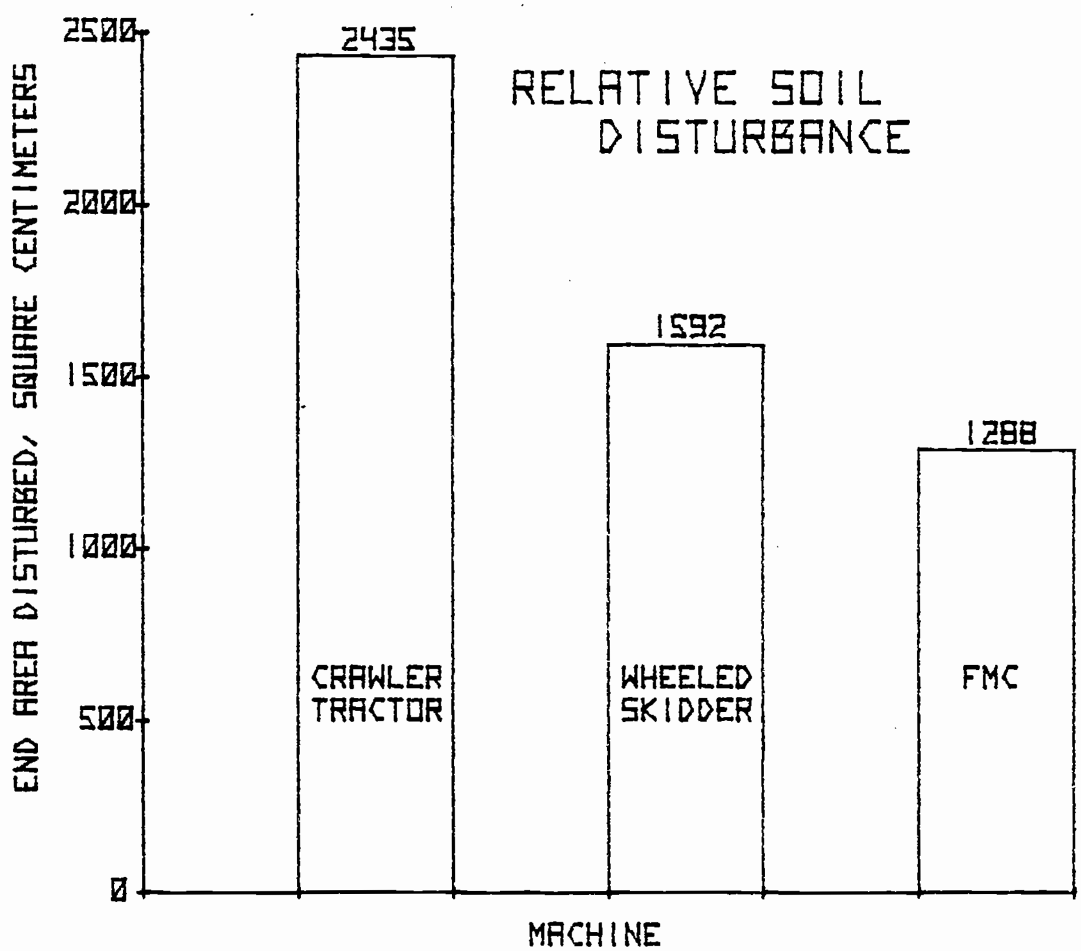

Figure 13. Relative soil disturbance by machine.

the center of the trail is easily explained as a result of soil mounding between the dragging logs. The soil accumulation in evidence along the outside edges of some trails occurs too frequently to be considered an error in data collection and is most likely the result of bearing capacity failures of the soil immediately beneath the track or tires. When failure occurs, soil is pushed up on either side of the failure. The bearing capacity failures are the result of numerous loadings of a pressure insufficient to cause a bearing capacity failure with only one loading.

Differences in soil disturbances between the three vehicle types may be explained by differences in suspension, track configuration, log suspension, constancy of ground contact, dynamic pressures, and load size.

The suspension systems for the two tracked vehicles are quite different. The track suspension system on the FMC is composed of five dual roadwheels supporting each track. Each roadwheel is independently sprung using a torsion bar system. The track can flex to form a concave surface with respect to the soil. The driving sprocket for the FMC is located forward of the five roadwheels. The track is slack as it is laid on the ground and is in tension between the rear idlers and the drive spocket. The slack track conforms to the soil surface. The track on the crawler tractor is rigidly suspended and the track shoe cannot flex downward to form a concave contact surface with respect to the soil. Soil surface disconformities tend to bear the entire tractor weight until they are crushed and flattened.

Track configuration may also be a factor in the differences observed in soil disturbance. The grousers on the FMC do not protrude as far as on the crawler tractor or the ribs on the tires of the wheeled skidder. The greater protrusions on the tractor and skidder will result in higher point loads than the more uniform FMC track.

The machines have different log suspension systems. The FMC supports the leading end of the log higher off the ground than the two other vehicles; therefore, the dragging logs have less ground contact area, possibly resulting in less soil displacement.

The wheeled skidder failed to maintain constant ground contact, unlike the tractor or FMC. The wheeled skidder was operated in two-wheel drive while travelling down the strips. This author observed bouncing over stumps even though the stumps were originally cut off close to ground level. While the skidder bounced, the drive wheels freely rotated. As the freely rotating wheels settled back onto the soil surface, high local pressures and resulting lateral forces were exerted on the soil which resulted in high local soil displacement.

Obvious differences were observed in machine operating velocity. The operating velocity affects the duration of impact. The FMC is capable of maintaining a higher speed than the crawler tractor under identical conditions, as specified in the equipment specification sheets. Assuming that the tractor generally operated at a velocity of 4.0 kilometers per hour (2.5 mph) in second gear, and an average load of 6,440 kilograms (14,200 lbs.), the tractor would be operating over a particular soil element for a duration of 2.4 seconds per loaded pass, or a total of 48 seconds for 20 loaded passes. Assuming a constant 6,440 kilograms average load, operation in second gear, and an operating velocity of 4.8 kilometers per hour (3.0 mph), the FMC would be over a soil element for a duration of 2.1 seconds for one loaded pass and a total of 42 seconds for 20 loaded passes. According to the above calculations, the tractor would be exerting compactive pressure and vibration to the soil for six more seconds for every 20 loaded passes than the FMC.

As detailed in Appendix B, differences in dynamic pressures were calculated for each machine. The crawler tractor exerted higher average maximum dynamic pressures than the skidder, 97.2 kilopascals versus 81.4 kilopascals (14.1 psi versus 11.8 psi), and more than the FMC's average 64.9 kilopascals (9.4 psi) dynamic pressure. The crawler tractor and the wheeled skidder both exerted higher overall average dynamic pressures, 77.2 kilopascals (11.2 psi) and 80.0 kilopascals (11.6 psi), respectively, than the FMC's 52.9 kilopascals (7.7 psi) average dynamic pressure.

In order to achieve satisfactory machine performance, differences in turn weights were allowed between machines. The average wheeled skidder turns were only 54 percent of the weight of the average crawler tractor and FMC turns; therefore, to skid the same volume of wood, the wheeled skidder would have to make 1.85 times as many trips as the crawler tractor or FMC. If soil disturbance continued at the same rate for the additional trips as for the first 20, the wheeled skidder would disturb approximately 2940 square centimeters of soil, approximately 500 square centimeters more soil disturbance than was observed with the crawler tractor. Since the amount of disturbance probably does not increase linearly after 20 trips, equal disturbance probably results from skidding comparable volumes of wood with either the crawler tractor or the wheeled skidder.

Two of the wheeled skidder profiles showed that soil was accumulated and compacted and not displaced and compacted, as is the case in all other profiles. The deposition of soil could be the result of sampling error, or the leading end of the log coming in contact with the soil as the machine bounced and thus locally depositing soil. It could also occur as a result of hard downward bouncing of the skidder on both sides of the profile, leading to local bearing capacity failures on either or both sides of the profile with resulting soil mounding across the profile location. Such bearing capacity failures from repeated passes probably caused the indicated soil accumulations on the outside edges of the strip evident on numerous profiles. The explanation for this apparent anomaly is not clear.

CONCLUSIONS

The Gus probe, a new tool designed to be durable and easy to use, failed to yield statistically significant predictive variables consistently between sites; therefore, the tool should not be adopted as designed. Because statistically significant predictor models were generated relating Gus variables to both density changes and cone penetrometer cone indices, a tool of similar design concepts, but different design dimensions, could possibly generate a consistent predictor model for soil compaction.

The cone penetrometer is a useful tool for predicting soil compaction resulting from the use of ground-based logging vehicles. The models generated should be validated prior to adoption, however.

Soil disturbance, defined in this paper to be a measure of both soil compaction and soil displacement, was markedly higher for the tractor than for the skidder or FMC. The skidder disturbed slightly more soil than the FMC. If the skidder were required to make the number of passes necessary to skid the same volume of wood as the tractor or FMC, the resulting disturbance would probably approach that of the tractor.

The measure of soil compaction should be change in soil densities, not the absolute value of density attained. The dense, slightly cohesive soil was compacted approximately equally by all machines at the five centimeter depth (2 in.), but was compacted more by the tractor at greater depths. The tractor caused obvious compaction even at the 30.5 centimeter depth. Little compaction was caused below the 15.2 centimeter (6 in.) depth by either the skidder or FMC on this dense, cohesive soil.

The loose slightly cohesive soil was compacted more by the tractor than by either the skidder or the FMC at all depths. Compaction decreased rapidly for the skidder and FMC below 20.3 centimeters (8 in.), but a similar decrease was not observed for the tractor. The loose, cohesionless soil was compacted less from the FMC at the five centimeter depth, but no obvious differences in soil compaction were observed at greater depths. The dense, cohesionless soil was compacted less by the skidder at the five centimeter depth, and only slightly more compaction for the FMC at the same depth, but no differences between machines at greater depths. Obvious differences were noted between absolute densities attained for each machine and the magnitude of the density changes, reflecting the differences in initial strip densities.

The machine derived pressures (Appendix B) found the highest calculated pressure to have occurred on the trailing edge of the tractor track. The highest average pressure occurred on the skidder. The FMC had both the lowest overall pressure, which occurred on the trailing edge of the track, and the lowest average pressure along the bottom of the tracks.

SUMMARY

The Gus probe failed to generate a statistically significant equation utilizing the same independent variables between sites; therefore, the tool is not recommended for use.

The cone penetrometer data yielded a statistically significant model to predict soil compaction resulting from the use of ground-based logging vehicles. All sites taken separately and all sites combined yielded a linear model in one variable. The model for all sites combined, significant at the .001 probability level, is: $n = 33$ $R^2 = .7339$

$$CD08 = 0.2631 - 0.0001022(CI6, \text{in kPa})$$

Or, in U.S. Customary Units:

$$\text{Density Change} = 16.42 - 0.04643\ (CI6, \text{in psi})$$

where:

CD08 = change in soil density to the 20.3 cm depth, $\frac{g}{cc}$

CI6 = cone index for 15.2 cm (6 in.) penetration of the penetrometer tip.

Density Change = change in soil density to the eight inch depth, lbs/ft^{-3}.

The soil compaction information is summarized in the Conclusion section of this report.

The soil disturbance profiles show the tractor disturbing an average of 2435 cm^2 (377 $in.^2$), the skidder disturbing an average

of 1529 cm^2 (245 $in.^2$), and the FMC disturbing an average of 1288 cm^2 (200 $in.^2$) of soil. The ratio of disturbances, respectively, is 1.9:1.2:1.0, setting the lowest disturbance at 1.0. The skidder turns averaged only 54% of the weight of the tractor and FMC turns.

The derived loaded vehicle pressure distributions on the bottom of the tracks and tires were calculated for each machine. The average pressures calculated for the skidder are 79 kPa (11.4 psi) on the front tires, and 82 kPa (11.8 psi) on the rear tires. The pressure distribution along the bottom of the track of the crawler tractor shows an average pressure of 57 kPa (8.3 psi) on the leading edge of the track and 97 kPa (14.1 psi) on the trailing edge of the track. The pressure distribution along the bottom of the track of the FMC shows an average pressure of 63 kPa (9.1 psi) on the leading edge of the track and 43 kPa (6.3 psi) on the trailing edge of the track. The average tractor/FMC turn weighed 6440 kg (14,200 lbs.). The average skidder turn weighed 3490 kg (7,700 lbs.).

SUGGESTIONS FOR FURTHER RESEARCH

The test strip length and width and the test plot length and width were adequate without being excessive in either dimension. The loaded piece of equipment should be able to enter the test strip easily. If the vehicle must stop to get aligned properly with the strip, random use of the full width of the strip is not encouraged. The strips should be laid out in metric units.

Further tests should expand the range of soils tested. Emphasis should be placed on testing more plastic soils and a gravelly soil to increase the range of applicability of the predictive model.

The machines used should continue to represent typical machines encountered in logging operations, as is the case in the current study. The machines should continue to be able to suspend the leading end of the log. Crawler tractor track widths and wheeled skidder tire sizes should be representative of sizes commonly encountered in logging operations. Maintaining constant tract and tire sizes between tests will permit isolating the effects of different soils without the introduction of new independent variables, however.

The log weights used in the study appeared to be satisfactory. The use of multiple log turns should be continued for all machines to provide continuity between tests. One log turns which fully utilize the machine power and traction capabilities are atypical.

The log weights should continue to be determined by weighing both ends of the log to permit determination of the log center of gravity. The choker attachment point should be established for each log and held constant, perhaps by notching the log. Knowing the choker attachment point would improve the accuracy of the derived pressure calculations.

The soil density measurements were taken at appropriate depths. The evidence of compaction at the 30.5 centimeter depth indicates some density measurements should have been taken at greater depths. The plot locations should represent the effects of the passage of the vehicle and turn of logs comparably between strips. The entirely random method of locating the density plots for this test resulted in an uneven distribution of plots across the width of the test plot. As a result, some trails possibly show more compaction than others because more density plots were taken in the center of the trail than along the edges. Plots located towards the center of the trail are impacted with every pass of the vehicle while plots located towards the edges of the trail are impacted only when the vehicle passes along the edge on which the plot is located. Distributing the density plots evenly across the width of the test plot for all strips would enhance the comparability between strips. The density plots should be located randomly along the longitudinal axis of the test plots.

The dynamic pressure distribution measurements could be easily enhanced by chokering the log at a constant distance from the end of the log, as previously discussed, and by collecting photographs taken perpendicularly to the loaded moving vehicle to obtain measurements of the choker angle. The vehicle should be passing through the test plot when the picture is taken. If the choker angle, angle "a" in Appendix B of this paper, can be determined with accuracy, the tension in the choker can be accurately determined, as can a check on the soil-log coefficient of friction. Additional tire print measurements should be taken for the wheeled skidder. The tire print measurements should be made with the tire lugs embedded in the soil and the flat tire surface supported on top of the soil. The measurements should be made on both the front and the rear tires under various log loads. If angle "a" cannot be naturally simulated, the free end of the logs should be chokered to an anchor and the skidder advanced until the choker angle approaches the angles computed in Appendix B. Knowing the exact tire contact area for various choker angles would improve the accuracy of the derived pressure calculations.

The soil disturbance profile technique seemed to work very well. Additional profiles should be taken to generate improved average data by averaging the effect of stumps or surface disconformities. Profile measurements should also be taken at ten trips to quantify the soil disturbance with increased trips and to perhaps detect the gradual formation of soil accumulations as a result of bearing capacity failures. Profile measurements should also be taken on the tractor and FMC trails after the number of passes of those machines which would be required to skid the same volume of wood as the wheeled skidder after 20 trips, thus permitting a comparison of soil disturbance between machines for an equal volume of wood skidded as well as for an equal number of trips. Calculating an average depth to the soil surface before and after skidding would give a fast estimate of whether soil was deposited or displaced. If soil appears to have been deposited, reasons should be immediately established for the deposition or the erroneous data corrected.

The cone penetrometer has been shown to be a statistically significant predictor of soil compaction resulting from the use of ground-based logging vehicles. Validation of the predictive model is required prior to its adoption. Further testing of the cone penetrometer should use smaller cone sizes in addition to the cone size used in the tests described in this paper. Sample depth should also be varied to establish an optimum depth. The cone index associated with the plastic deformation loading on the proving ring should be used for samples in which the desired depth could not be attained due to roots, rocks or hard soil.

The Gus probe was conceived to be an easy to use indestructable tool which could predict soil compaction resulting from the use of ground-based logging vehicles. Although the tool failed to generate a useful predictive equation the goals which lead to the design of the tool remain. A new tool based on the design of the Gus probe could potentially prove to be a significant and useful predictor. The tool should be designed to facilitate simple data gathering procedures, thus eliminating all data which requires recording penetration per blow. Total penetration for a fixed number of blows or blows to attain various depths are easy to measure variables and should be stressed. Further design concepts are itemized in the Comparison of the Gus Probe and the Cone Pentrometer section of this report.

BIBLIOGRAPHY

Bell, J.R. 1977. Preliminary Study of Compaction Energy Relationships of Cohesive Soils. A paper presented at the annual meeting of the Transportation Research Board, Washington, D.C.

Bradshaw, G.R. 1979. The Effect of Preplanned Skid Trails and Winching on a Partial Cut. A paper submitted to Oregon State University in partial fulfillment of the requirements for the degree Master of Forestry.

Falk, G.D. 1981. A Study of the Lateral Yarding Forces in a Cable Thinning. A Thesis submitted to Oregon State University in partial fulfillment of the requirements for the degree Master of Science.

Froehlich, H.A. 1974. Soil Compaction: Implication for Young-Growth Management. Proceedings, Managing Young Forests in the Douglas-fir Region Symposium. 4:48-63.

Froehlich, H.A. 1978a. Soil Compaction from Low Ground-Pressure, Torsion-Suspension Logging Vehicles on Three Forest Soils. Oregon State University Forest Research Laboratory Research Paper 36.

Froehlich, H.A. 1978b. The Physical Effects of Timber Harvesting on Forest Soils. Proceedings, Society of American Foresters, Albuquerque, New Mexico.

Hatchell, G.E., C.W. Ralston, and R.R. Foil. 1970. Soil Disturbances in Logging. Journal of Forestry 68(12):772-775.

Henshaw, J.R. 1977. A Study of the Coefficient of Drag Resistance in Yarding Logs. A Thesis submitted to Oregon State University in partial fulfillment of the requirements for the degree Master of Science.

Lull, H.W. 1959. Soil Compaction on Forest and Range Lands. U.S. Department of Agriculture Miscellaneous Publication 768.

Meriam, J.L. 1978. <u>Statics</u>. John Wiley and Sons, Inc. New York. 398 p.

Pritchett, W.L. 1979. <u>Properties and Management of Forest Soils</u>. John Wiley and Sons, Inc. New York. 500 p.

Raghavan, G.S.V., E. McKyes, I. Amir, and R.S. Broughton. 1976. Prediction of Soil Compaction Due to Off-Road Vehicle Traffic. Transactions of the ASAE Vol. 19, No. 4:610-613.

Steinbrenner, E.C. 1955. The Effect of Repeated Tractor Trips on the Physical Properties of Forest Soils. Northwest Science Vol. 29, No. 4:155-159.

Weaver, H.A. and V.C. Jamison. 1951. Effects of Moisture on Tractor Tire Compaction of Soil. Soil Science 71:15-23.

APPENDICES

APPENDIX A

CALIBRATION OF THE CONE PENETROMETER

A cone penetrometer is composed of a 30 degree circular stainless steel smooth cone which is driven into the soil by a shaft. The shaft is connected through a proving ring to a handle shaped to facilitate exerting the high pressures required to push the cone into the soil. A dial is mounted on the proving ring to measure deflection of the ring with increased force on the handle. The dial reading may be correlated with force exerted on the top of the handle or to cone index, the force divided by the end area of the penetrometer cone. The unit of measure for cone index is pounds per square inch, expressed as a function of depth to which the cone is pushed. In this paper cone index is expressed as the pressure required to push the cone tip to the 10.2 cm (4 in.) and 15.2 cm (6 in.) depths, as measured to the tip of the cone. Because a 5.08 cm (2.0 in.) cone was used throughout the tests, the cone indices correspond to penetrations of 5.1 cm (2 in.) and 10.2 cm (4 in.) from the cone shoulders.

To calibrate the dial readings to cone index, the dial was reset to zero while freely suspending the penetrometer from the handle. The penetrometer was then lowered onto a block of wood to prevent injury to the penetrometer tip. At this point the proving ring was deflected to indicate the weight of the handle and the dial reading recorded for an external loading of zero pounds. Additional weight was then added to the handle in measured increments of approximately 2.3 kg (5 lbs.) each and the dial reading recorded. Increments of weight were added up to a total weight of 84 kg (185 lbs.).

The penetrometer cone, being a 30 degree cone 5.08 cm (2.0 in.) high, has an end area of 5.82 square cm (0.902 in.^{2}). The cone penetrometer weighs 2.60 kg (5.74 lbs.). Therefore, with no external loading on the vertically oriented penetrometer, the cone index would be 2.60 kg (5.74 lbs.) divided by 5.82 cm^2 (0.902 in.^{2}), or 43.9 kPa (6.36 psi). Subsequent cone indices were calculated by adding the 2.60 kg (5.74 lbs.) penetrometer weight to the imposed external loading on the handle and dividing by the 5.82 cm^2 (0.902 in.^{2}) cone end area.

Regressing the independent variable of penetrometer dial reading against the dependent variable of cone index for 30 observations resulted in the following equation, pertinent only to the penetrometer used in this study, in U.S. Customary Units:

cone index = 1.53 + 0.308 (dial reading)

The coefficient of determination is 1.00. The cone indices obtained in this manner were used in this paper, in units of pounds per square inch.

APPENDIX B

CALCULATION OF MACHINE DERIVED PRESSURES

ASSUMPTIONS

The calculations for machine derived pressure are based on the following assumptions:

1. The soil/log coefficient of friction is a constant equal to 0.6 (Henshaw, 1977 and Falk, 1980). The coefficient of friction does not vary with soil moisture content.
2. The ground-based logging vehicles were operated with constant velocity, thus permitting use of equations of equilibrium for both the logs and the skidding machines. The strips were planned to facilitate maintenance of a constant velocity.
3. The multiple log turns can be approximated by a single log turn of equal end weights and equal total weights.
4. The leading end of the logs being skidded were elevated; therefore, the effects of plowing of the leading end of the logs were eliminated. The chokers were tensioned to ensure leading end suspension.
5. The largest end of the log is the leading end.
6. The choker can be assumed to be attached at the end of the log except for the calculations for the FMC, where a support point two feet from the large end of the log is used.
7. The log is a rigid body and the log diameter is neglible when compared with the length.

8. Coulomb friction exists between the log and the soil.
9. The rollers and track of the FMC may be analyzed as a rigid frame even though the rollers are actually independently torsion bar suspended.
10. The deflection of the tires of the wheeled-skidder remains constant regardless of loading.
11. The derived pressure on the bottom of the tires of the skidder can be approximated by dividing the normal force on the tire by the ground contact area. The effects of the tire ribs are ignored.

Although errors are introduced by the preceeding assumptions, the magnitude of the errors introduced, in the opinion of this author, is less than the variability in topography, soil moisture content, machine velocity, etc., normally encountered in actual skidding operations.

FORCE ANALYSIS OF A SKIDDED LOG

In order to determine the pressure distribution along the bottom of a tracked vehicle or on the tires of a rubber-tired vehicle, one needs to know the line tension and angle of pull of the bull line between the skidding machine and the logs being skidded.

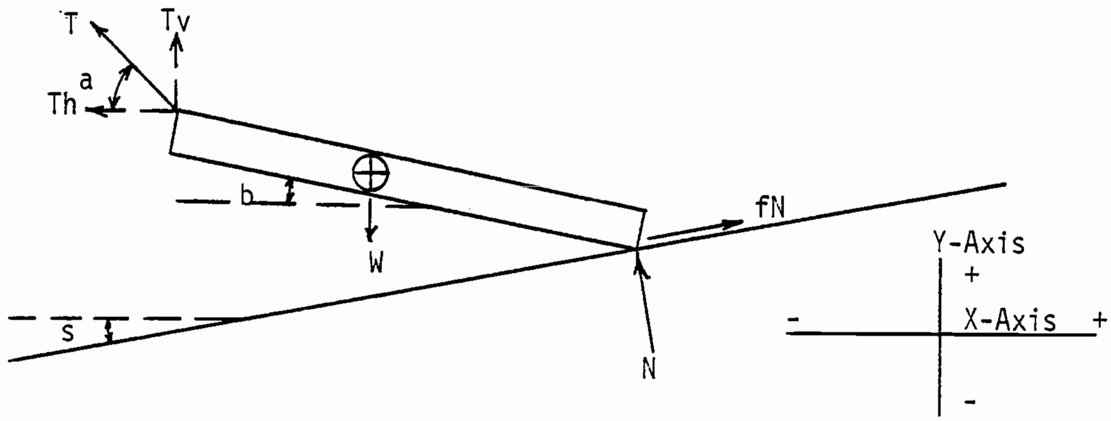

Figure 14. Free body diagram of a skidded log.

where:

T = Tension, in pounds, of the bull line to the piece of equipment doing the skidding.

Tv = Vertical component of T.

Th = Horizontal component of T.

W = Log weight, in pounds.

Ws = Weight of the small end of the log, in pounds.

WL = Weight of the large end of the log, in pounds.

a = Angle of pull of T, in degrees, measured from the horizontal.

N = Normal component, in pounds, on the dragging end of the log.

f = Coefficient of friction between the log and the soil.

fN = Force resisting skidding, in pounds, parallel to the soil surface.

s = Slope angle, in degrees, measured from the horizontal (downslopes in the direction of skidding are entered as negative degrees).

b = Log angle, in degrees, measured from the horizontal (downslopes in the direction of skidding are entered as negative degrees).

Using the equilibrium equations of motion:

$$\Sigma Fx = 0 = fN\cos s + N\sin s - T\cos a$$

Solving for Tcos a:

$$T\cos a = fN\cos s + N\sin s \qquad (1)$$

$$\Sigma Fy = 0 = T\sin a - W + N\cos s - fN\sin s$$

Solving for Tsin a:

$$T\sin a = W - N\cos s + fN\sin s \qquad (2)$$

Equations (1) and (2) are two equations in two unknowns, T and a.

Solving for T in terms of a:

(2) $$T = \frac{W - N\cos s + fN\sin s}{\sin a} \qquad (3)$$

Substituting the equation for T into equation (1):

$$\frac{\cos a\,(W - N\cos s + fN\sin s)}{\sin a} = fN\cos s + N\sin s$$

Solving for a:

$$a = \tan^{-1}\left[\frac{W - N\cos s + fN\sin s}{fN\cos s + N\sin s}\right]$$

Assumption number one sets a constant value for f of 0.6. Also, setting: N = Ws Cos s, a good approximation, yields an expression for "a" in terms of known values:

$$a = \tan^{-1}\left[\frac{W - Ws\cos^2 s + 0.6Ws\ (\cos s)(\sin s)}{0.6Ws\cos^2 s + Ws\ (\cos s)(\sin s)}\right] \quad (4)$$

Substituting the above approximation for N into (3) yields an expression for T given "a" and "f:"

$$T = \frac{W - Ws\cos^2 s + 0.6Ws\ (\cos s)(\sin s)}{\sin a} \quad (5)$$

Equations (4) and (5) permit solving for the line tension and angle of pull of the bull line between the skidding machine and the turn. Fortunately, the log weights for the compaction study were obtained by weighing each log end separately; therefore, the total log weight and the weight of each end of the log is known. Normally, this data is not known. Estimates of the total log weight may be obtained by use of one of the many local conversion factors relating log weight to log volume. The weight of the small end of the log may be estimated from the product of total log weight and the ratio of the small end diameter to the log large end diameter.

One should also remember at this point that the values obtained for "T" and "a" represent static equilibrium in which the ground slope, soil-log coefficient of friction, topography, direction of travel, and machine velocity remain constant. The values for "T" and "a" represent a hypothetical situation which would seldom be attained at any given point in time in an actual skidding operation. The values of "T" and "a" can be characterized as averages. The magnitude of the errors introduced in the assumptions required to calculate "T" and "a," in the opinion of this author, are less than the magnitude of the errors introduced by assuming static equilibrium.

The following table lists the pertinent machine parameters required to establish dynamic loadings.

TABLE VIII. MACHINE PARAMETERS FOR ESTABLISHING DERIVED PRESSURES.

PARAMETER	CRAWLER TRACTOR	FMC	WHEELED SKIDDER
Xc	39.4	39	36.2
Yc	33.2	40	42.0
Xp	141.1	79	133.3
Yp	48.3	96	91.2
W	39240	29440	19980
L	106	113	113
w	20	22	----
A	4240	4972	1048

Xc = Horizontal distance measured from a perpendicular from the centerline of the front sprocket (or roadwheel) to the ground to the vehicle center of gravity, in inches.

Yc = Vertical coordinate measured upward from the bottom of the track faces for the crawler tractor and the FMC and upward from the bottom of the deflected wheeled skidder tire to the vehicle center of gravity, in inches.

Xp = Horizontal distance aft of the centerline of the front sprocket (or roadwheel) to the arch fairlead, in inches.

Yp = Vertical distance upward from the bottom of the track faces for the tracked vehicles and upward from the bottom of the deflected rubber tire for the wheeled skidder to the arch fairlead, in inches.

W = Actual machine weight for the specific machines used in the study, in pounds.

L = Track length in contact with the ground as given in the equipment specification sheets for the tracked vehicles and wheelbase of the wheeled skidder, in inches.

w = Track width as given in the equipment specification sheets for the tracked vehicles, in inches.

A = Track area in contact with the ground, as found by multiplying L·b and summing for each track. The ground contact area for the wheeled skidder was determined by actual field measurements of the deflected tire in soil of such consistency that the tire ribs were embedded in the soil, but the flat tire surface was supported on top of the soil. Units are square inches for two tires.

The center of gravity data was obtained from telephone conversations with the respective company representatives and engineers. The center of gravity for the wheeled skidder was determined by the rear axle centerline tipping method using deflected tire radius.

The coordinates of the fairlead were determined from known vehicle dimensions from vehicle specification sheets and readily available dimensions. Scaling from known parameters was used as required. The fairlead location for the FMC was established as the top of the fairlead on the carrier arch, a simplification of the actual coordinates for the reaction of the log on the vehicle. The simplification assumes the friction of the log on the machined metal of the carrier is neglible and all of the log-soil skidding resistance is passed through the bull line and the fairlead. The previous assumption will have the effect of shifting the resultant of the soil pressure distribution along the bottom of the track rearward. Another assumption inherent in using the fairlead as the location of the reaction on the vehicle is that the vertical support for the log acts through the fairlead and not on the carrier arch in conjunction with the fairlead. The second assumption has the affect of shifting the resultant of the soil pressure distribution along the bottom of the track forward. While the effects of the assumptions act to shift the location of the resultant of the track pressure distribution in opposite directions, this author does not mean to imply that the overall effects are offsetting.

DERIVED LOADING OF A WHEELED SKIDDER

The derived loading of the tires of a wheeled skidder may be determined by considering a free body diagram of a skidder.

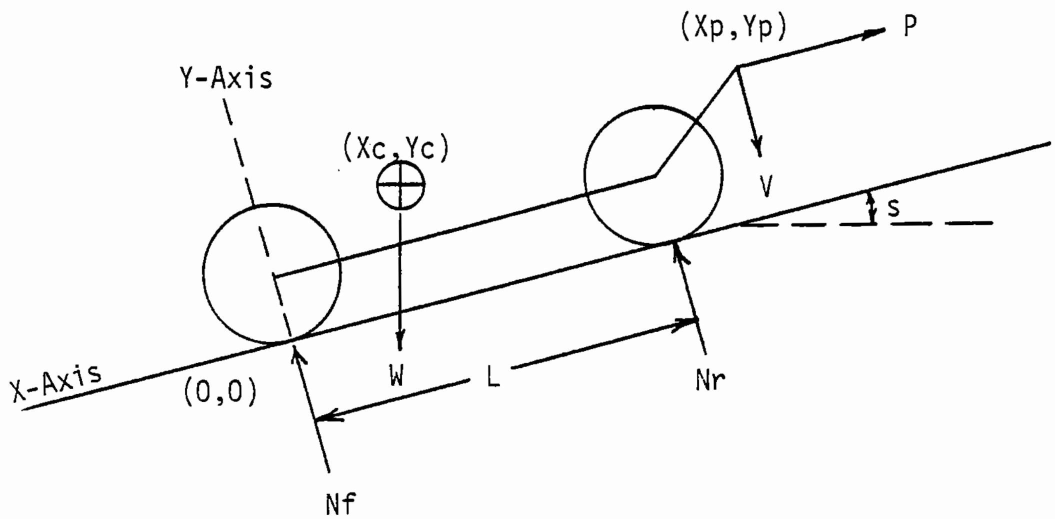

Figure 15. Free body diagram of a wheeled skidder.

where:

Nf = Normal force on the two front tires, in pounds.

Nr = Normal force on the rear two tires, in pounds.

Pf = Pressure on each front tire, in pounds per square inch.

Pr = Pressure on each rear tire, in pounds per square inch.

L = Wheelbase of the wheeled skidder, in inches.

P = Pull parrallel to the ground, a component of the tension, T, in the bull line, in pounds.

V = Pull perpendicular to the ground, a component of the tension, T, in the bull line, in pounds.

s = Ground slope, in degrees, as defined previously.

W = Actual machine weight, in pounds.

Using equilibrium equations of motion (clockwise positive):

$$\Sigma Mf = 0 = PYp + VXp + WXc\cos s + WYc\sin s - NrL$$

Solving for Nr:

$$Nr = \frac{PYp + VXp + WXc\cos s + WYc\sin s}{L} \qquad (6)$$

$$\Sigma Mr = 0 = NfL - W(L-Xc)\cos s + WYc\sin s + PYp - V(L-Xp)$$

Solving for Nf:

$$Nf = \frac{W(L-Xc)\cos s - WYc\sin s - PYp + V(L-Xp)}{L} \qquad (7)$$

From the geometry of the free body diagram of a skidded log:

$$P = T\cos(a-s) \qquad (8)$$

$$V = T\sin(a-s) \qquad (9)$$

Also, dividing the loadings for the two tires, Nf and Nr, by the ground contact surface area for the two tires yields an approximation of the ground pressure on the tires:

$$Pr = \frac{Nr}{1048} \qquad (10)$$

$$Pf = \frac{Nf}{1048} \qquad (11)$$

Applying equations (3) and (4) and equations (6) through (11) yields the data in the following table.

TABLE IX. DERIVED WHEEL PRESSURES FOR THE WHEEL SKIDDER.

	Degrees		Pounds			psi		kPa	
Strip	a	s	T	P	V	Pf	Pr	Pf	Pr
M3	64	-1	5845	2470	5297	10	14	69	97
M4	63	+1	5999	2816	5297	10	14	69	97
M9	66	-5	5566	1812	5263	11	13	76	90
B1	64	-2	4514	1836	4124	11	12	76	83
B6	64	-3	4457	1741	4103	11	12	76	83
B8	66	-5	4351	1417	4114	12	11	83	76
P3	67	-3	3658	1251	3437	12	11	83	76
P5	66	-2	3699	1386	3430	12	11	83	76
P9	66	-2	3699	1386	3430	12	11	83	76
Y1	72	-5	4471	1006	4356	12	11	83	76
Y5	72	-6	4436	922	4339	12	11	83	76
Y9	72	-6	4436	922	4339	12	11	83	76

DERIVED TRACK LOADING OF A TRACKED VEHICLE

The derived pressure distribution along the bottom of the track of a tracked vehicle can be obtained by considering the following free body diagram of the tracks and arch of a tracked vehicle.

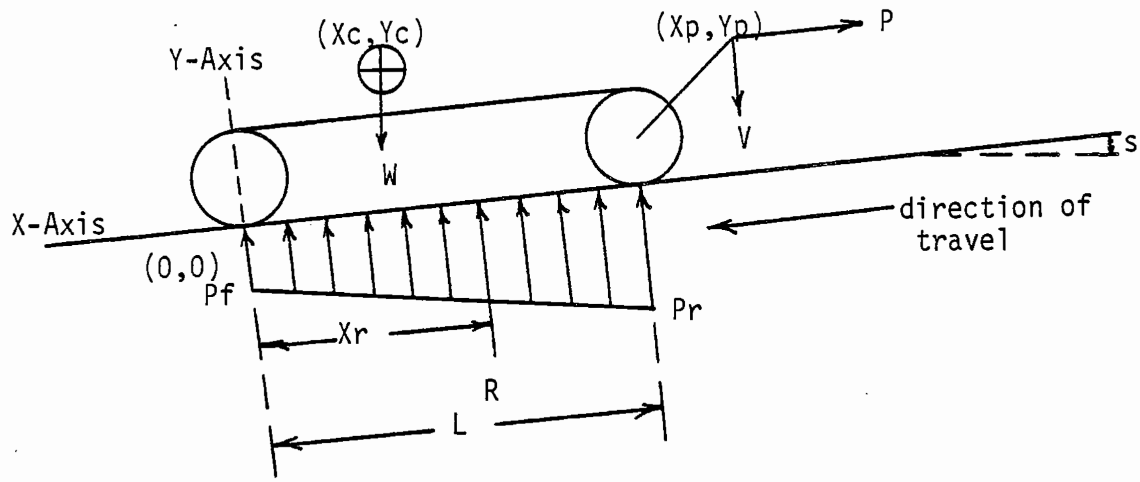

Figure 16. Free body diagram of a tracked vehicle.

where:

L, P, V, s = As previously defined for the wheel skidder.

R = Resultant force from the soil acting on the bottom of the tracks, in pounds.

Xr = Location of the resultant of the pressure distribution acting on the bottom of the tracks, measured aft of the leading wheel parallel to the soil surface, in inches.

Pf = Pressure on the leading edge of each track, in psi.

Pr = Pressure on the trailing edge of each track, in psi.

The location of the resultant will affect the solution procedure. The resultant may be located in one of three situations with respect to track length:

1. $\frac{Xr}{L} < \frac{1}{3}$ (Figure 17)

2. $\frac{1}{3} \leq \frac{Xr}{L} \leq \frac{2}{3}$ (Figure 18)

3. $\frac{Xr}{L} > \frac{2}{3}$ (Figure 19)

The resultant of a triangular pressure distribution is located 1/3 of the distance along the distribution, measured from the highest pressure towards the point of zero pressure (Meriam, 1978). The first situation may be diagrammed as follows:

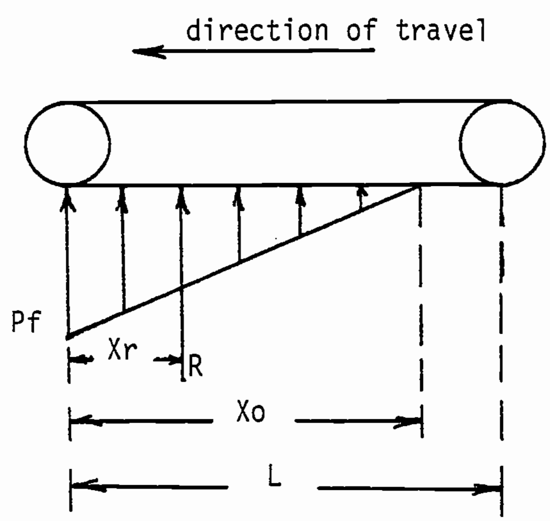

Figure 17. Pressure Distribution of $\frac{Xr}{L} < \frac{1}{3}$.

The above situation is likely to occur when descending a steep skid trail with a light log load. This situation was not encountered in the tests; however, the equations required to characterize the pressure distribution will be derived.

where:

Xo = Distance along track to the termination of the pressure distribution, in inches.

The second situation may be diagrammed as follows:

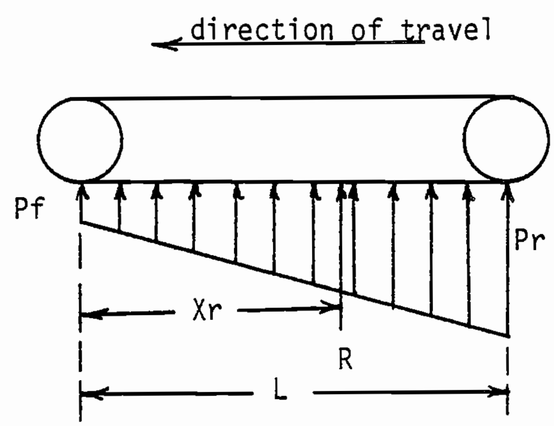

Figure 18. Pressure distribution of $\frac{1}{3} \leq \frac{Xr}{L} \leq \frac{2}{3}$.

Figure 18 shows Pr being greater in magnitude than Pf. This may not always be the case. Pf may be greater than Pr. The equations which characterize this pressure distribution will still pertain.

The third situation may be diagrammed as follows:

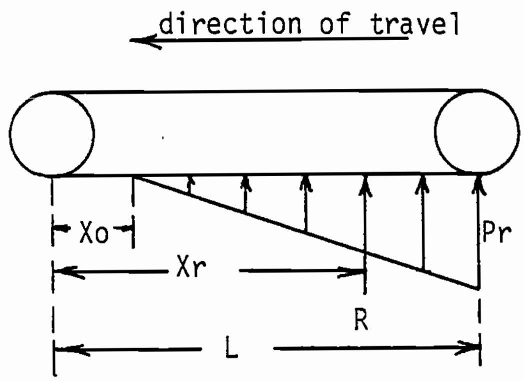

Figure 19. Pressure distribution of $\frac{Xr}{L} > \frac{2}{3}$.

Referring to Figure 16 and writing appropriate equilibrium equations of motion, the parameter required to characterize the pressure distribution along the bottom of the tracks of a tracked logging vehicle may be obtained.

$\Sigma Fy = 0 = R - W\cos s - V$

Solving for R:

$$R = W\cos s + V \qquad (12)$$

Setting "clockwise" moments as positive yields:

$\Sigma Mo = 0 = WXc\cos s + WYc\sin s + VXp + PYp - RXr$

Solving for Xr:

$$Xr = \frac{W\ Xccos\ s + WYcsin\ s + VXp + PYp}{R} \tag{13}$$

Now, substituting equation (9) into equation (12) and solving for R, one can solve for Xr and construct the ratio $\frac{Xr}{L}$ to determine which situation, situation 1, 2, or 3 applies.

If situation 1 applies, values for R and Xr are known. Equations for Xo and Pf must be obtained. A free body diagram of the pressure distribution on the soil surface is required.

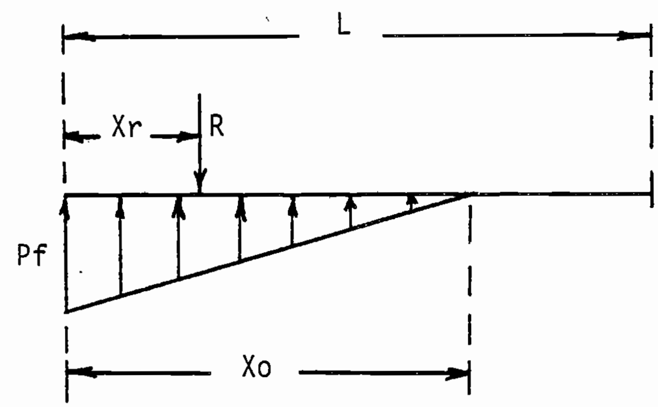

Figure 20. Free body diagram of track bottom, $\frac{Xr}{L} < \frac{1}{3}$.

Because the value for Xr is known from equation (13) the value for Xo can be found directly. The resultant of a triangular pressure distribution is located 1/3 of the distance along the distribution, measured from the highest pressure to the point of zero pressure (Meriam, 1978).

$$Xo = 3Xr \tag{14}$$

Setting "clockwise" moments around the left end of the track as positive yields:

$$\Sigma Mo = 0 = RXr - 1/2(Pf)(Xo)(2w)[\frac{Xo}{3}]$$

Simplifying and solving for Pf:

$$Pf = \frac{3RXr}{bXo^2} \tag{15}$$

Substituting the term for Xo in equation (14) into equation (15) and simplifying yields:

$$Pf = \frac{R}{3bXr} \tag{16}$$

If situation 2 applies, values for R and Xr are known. Equations for Pf and Pr must be derived. A free body diagram of the pressure distribution on the soil surface is required.

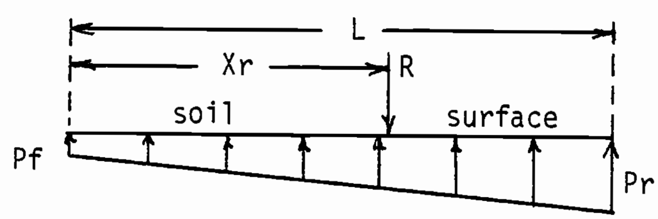

Figure 21. Free body diagram of track bottom, $\frac{1}{3} \leq \frac{Xr}{L} \leq \frac{2}{3}$.

Writing the appropriate statics equations for the surface area for both tracks:

$$\Sigma Fy = 0 = Pf(2wL) + 0.5(Pr-Pf)(2wL) - R$$

Solving for R:

$$R = PfwL + PrwL \tag{17}$$

Setting clockwise moments around the point of action of Pf to be positive yields:

$$\Sigma Mo = 0 = RXr - Pf(2wL)(0.5L) - .05(Pr-Pf)(2wL)(\frac{2L}{3})$$

Simplifying and solving for RXr:

$$RXr = \frac{wL^2}{3} \ (Pf+2Pr) \tag{18}$$

Solving equation (17) for Pf in terms of Pr and substituting the expression for Pf into equation (18) permits the derivation of an equation for Pr:

$$Pr = (\frac{3R}{wL})(\frac{Xr}{L} - \frac{1}{3}) \tag{19}$$

Substituting the equation for Pr, equation (19), into equation (17) permits deriving an equation for Pf:

$$Pf = (\frac{3r}{wL})(\frac{2}{3} - \frac{Xr}{L}) \tag{20}$$

If the ratio of $\frac{Xr}{L}$ indicates that situation three applies, values for Xo and Pr must be obtained. A free body diagram of the pressure distribution on the soil surface is required.

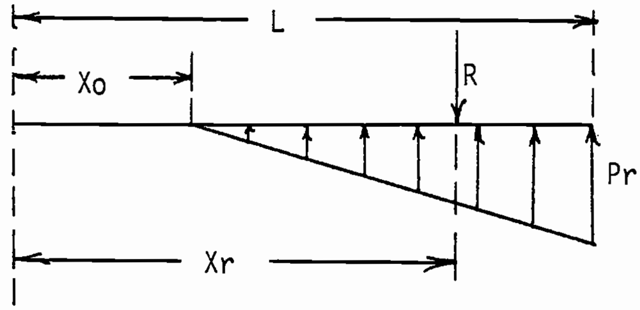

Figure 22. Free body diagram of track bottom, $\frac{Xr}{L} > \frac{2}{3}$.

Applying the appropriate equations of equilibrium:

$$\Sigma Fy = 0 = R - \frac{1}{2}(Pr)(b)(2)(L-Xo)$$

Solving for Pr:

$$Pr = \frac{R}{b(L-Xo)} \tag{21}$$

Setting "clockwise" moments taken around the left end of the track as positive yields:

$$\Sigma Mo = 0 = RXr - \frac{1}{2} Prb(L-Xo)[Xo + \frac{2}{3} (L-Xo)](2)$$

Solving for RXr and simplifying:

$$RXr = Prb(L-Xo)(\frac{2}{3}L + \frac{1}{3}Xo) \tag{22}$$

Combining equations (21) and (22) permits a solution for Xo:

$$Xo = 3L(\frac{Xr}{L} - \frac{2}{3}) \tag{23}$$

Substituting equation (23) into equation (21) yields an expression for Pr:

$$Pr = \frac{R}{3bL(1-\frac{Xr}{L})} \qquad (24)$$

Now, applying equations (3) and (4), equations (8) and (9), and equations (12) through (24), the pressure distribution along the bottom of the tracks of the crawler tractor may be described according to the machine parameters listed in Table X.

TABLE X. DERIVED TRACK PRESSURES FOR THE CRAWLER TRACTOR.

Strip	Deg.	Pounds		Inches		psi		kPa	
	s	P	V	Xr	Xr/L	Pf	Pr	Pf	Pr
M1	-1	4182	8986	62.07	0.59	6	17	41	117
M5	+1	4763	8958	63.55	0.60	5	18	34	124
M7	-4	3266	8972	59.75	0.56	7	16	48	110
B3	-3	3249	8042	58.60	0.55	8	15	55	102
B4	-4	2931	8054	57.83	0.55	8	14	55	97
B7	-6	2450	8013	56.35	0.53	9	13	62	90
P2	-3	2644	7264	56.59	0.53	9	13	62	90
P6	-2	2800	7295	57.28	0.54	8	14	55	97
P8	-3	2644	7264	56.59	0.53	9	13	62	90
Y3	-8	1321	7489	53.30	0.50	11	11	76	76
Y4	-5	2018	7532	55.49	0.52	9	13	62	90
Y8	-7	1594	7498	54.06	0.51	10	12	69	83

Log skidding with an FMC permits an exact analysis of the log skidding geometry because the log is firmly positioned on the carrier of the machine. Therefore, improved accuracy is possible in determining the log dragging forces. The geometry of the FMC is such that the typical 33 foot long log used in the tests forms a seven degree angle with the ground surface when the log is positioned properly on the carrier arch. The log angle is designated "b" in Figure 14. Knowing the exact value of "b" permits solving for the exact normal component on the log by considering the equations of equilibrium of a dragging log. As discussed previously, the support for the log on the arch is assumed to be located at a point two feet from the suspended large end of the log. I define a parameter, e, to relate the distance measured along the log from the support point to the center of gravity to the length of the log behind the support point.

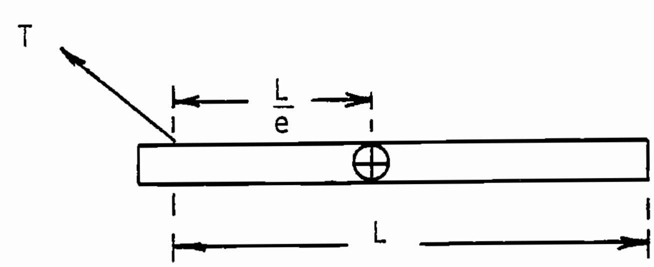

Figure 23. Relationship of support point to log center of gravity.

The value for "e" may be obtained by dividing the log length behind the support point by the distance from the support point to the center of gravity. The values for "e" are given in Table XI. A weighted length was used in the calculations for "e" for the logs on Yuba Pass, the only site with a log longer than 33 feet.

Referring to Figure 12 and the previous definition of "e" and taking clockwise moments around the point of choker attachment as positive yields the following equilibrium equation of motion:

$$\Sigma M = 0 = W(\frac{L}{e}) \cos (s+b) - LN\cos b - LfN\sin b$$

Solving for the normal component on the log yields:

$$N = \frac{W(\frac{L}{e}) \cos (s+b)}{L\cos b - Lf\sin b} \qquad (25)$$

Also,

$$\Sigma Fx = 0 = fN\cos s + N\sin s - Th$$

Solving for Th:

$$Th = N(f\cos s + \sin s) \qquad (26)$$

$$\Sigma Fy = 0 = Tv - W + N\cos s - fN\sin s$$

Solving for Tv:

$$Tv = W - N(\cos s + f\sin s) \qquad (27)$$

Equations (26) and (27) may be used to determine the magnitude of T. Given T, equations (8) and (9) and equations (12) through (24) yield the description of the derived pressure along the bottom of the tracks of the FMC contained in Table XI.

TABLE IX. DERIVED TRACK PRESSURES FOR THE FMC.

Strip	s	e	Pounds P	Pounds V	In. Xr	Xr/L	psi Pf	psi Pr	kPa Pf	kPa Pr
M2	-1	2.57	3272	10525	56.88	0.50	8	8	54	57
M6	+1	2.57	3827	10303	59.13	0.52	7	9	47	63
M8	-5	2.57	2098	10933	52.32	0.46	10	6	68	43
B2	-3	2.53	2490	9634	53.42	0.47	9	7	63	45
B5	-3	2.53	2490	9634	53.42	0.47	9	7	63	45
B9	-5	2.53	1949	9816	51.19	0.45	10	6	70	39
P1	-3	2.72	1950	8613	51.37	0.45	10	6	67	38
P4	-2	2.72	2176	8537	52.42	0.46	9	6	64	41
P7	-3	2.72	1950	8613	51.37	0.45	10	6	67	38
Y2	-4	2.85	1609	8919	50.21	0.44	10	5	71	35
Y6	-6	2.85	1136	9049	48.08	0.43	11	4	77	29
Y7	-6	2.85	1136	9049	48.08	0.43	11	4	77	29

APPENDIX C

SOIL END AREA DISTURBANCE PROFILES

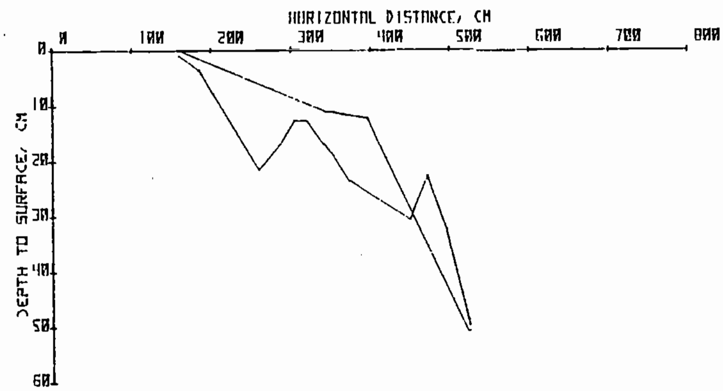

SKID TRAIL PROFILE AREA DISTURBED = 1712.87 SQ CM
MOONSHINE
TRACTOR
HIGH MOISTURE CONTENT
STRIP NO. 1

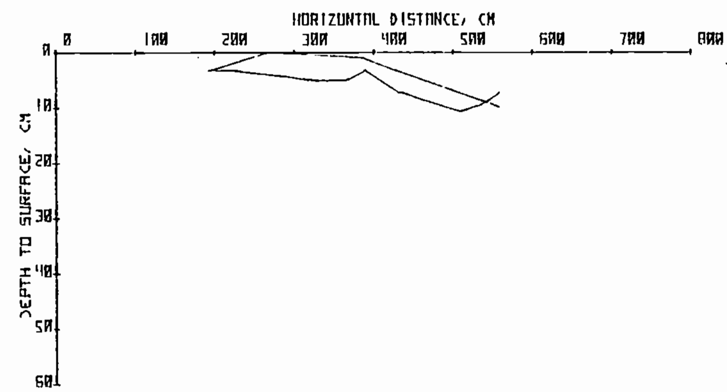

SKID TRAIL PROFILE AREA DISTURBED = 1073 SQ CM
MOONSHINE
FMC-210CA
HIGH MOISTURE CONTENT
STRIP NO. 2

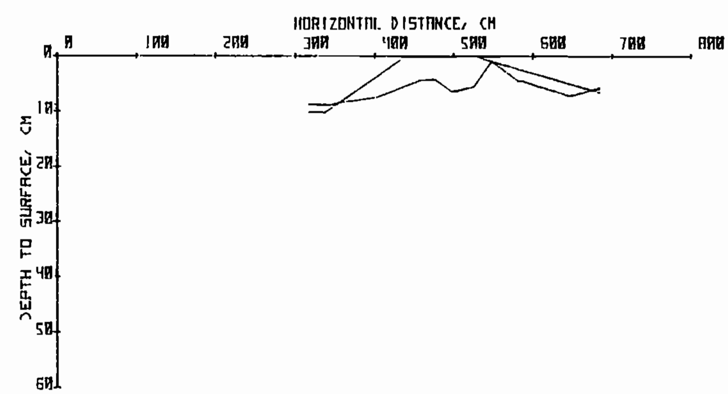

SKID TRAIL PROFILE AREA DISTURBED = 987.11 SQ CM
MOONSHINE
SKIDDER
HIGH MOISTURE CONTENT
STRIP NO. 3

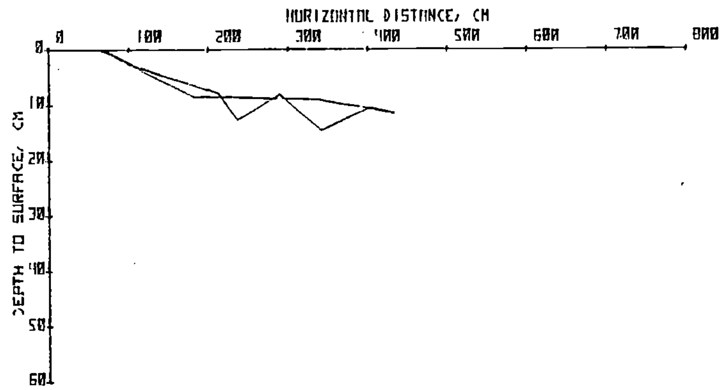

SKID TRAIL PROFILE   AREA DISTURBED = 259.215   SQ CM
MOONSHINE
SKIDDER
LOW (INTER) MOISTURE CONTENT
STRIP NO. 4

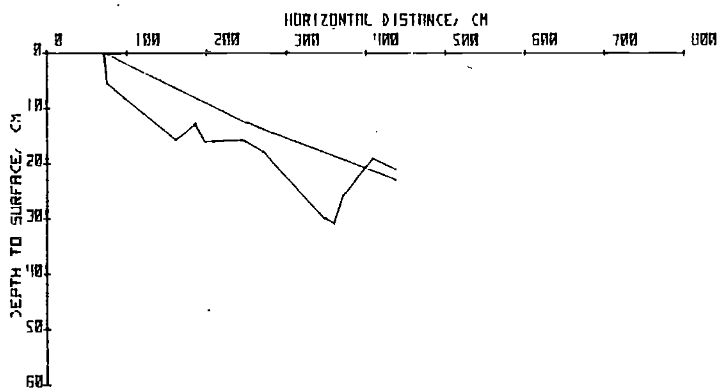

SKID TRAIL PROFILE   AREA DISTURBED = 2106.32   SQ CM
MOONSHINE
TRACTOR
LOW (INTER) MOISTURE CONTENT
STRIP NO. 5

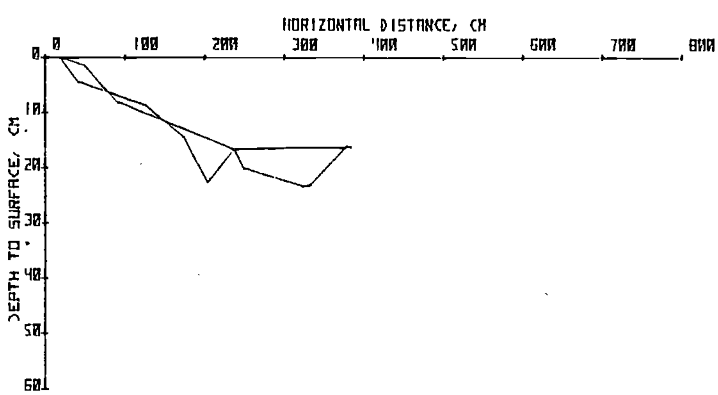

SKID TRAIL PROFILE   AREA DISTURBED = 962.705   SQ CM
MOONSHINE
FMC-210CA
LOW (INTER) MOISTURE CONTENT
STRIP NO. 6

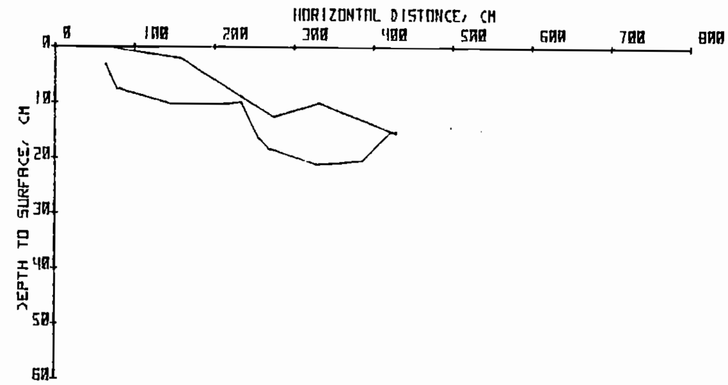

SKID TRAIL PROFILE AREA DISTURBED = 2360.67 SQ CM
MOONSHINE
TRACTOR
INTERMEDIATE MOISTURE CONTENT
STRIP NO. 7

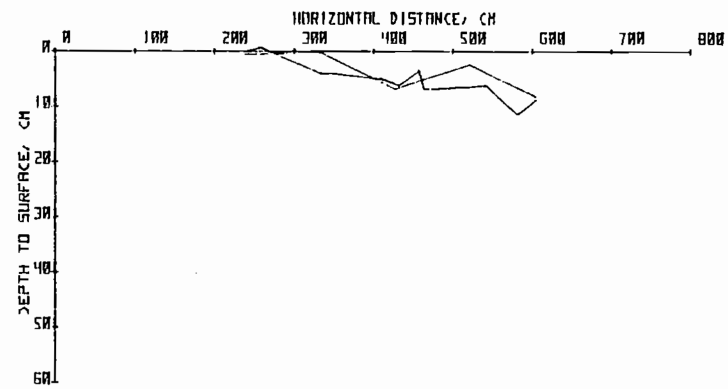

SKID TRAIL PROFILE AREA DISTURBED = 595.665 SQ CM
MOONSHINE
FMC-210CA
INTERMEDIATE MOISTURE CONTENT
STRIP NO. 8

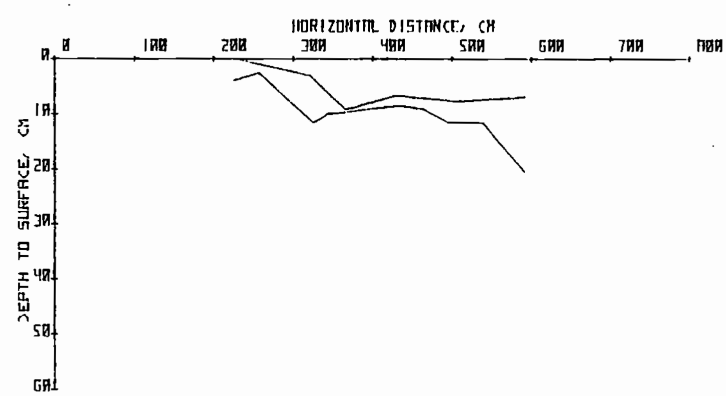

SKID TRAIL PROFILE AREA DISTURBED = 1419.215 SQ CM
MOONSHINE
SKIDDER
INTERMEDIATE MOISTURE CONTENT
STRIP NO. 9

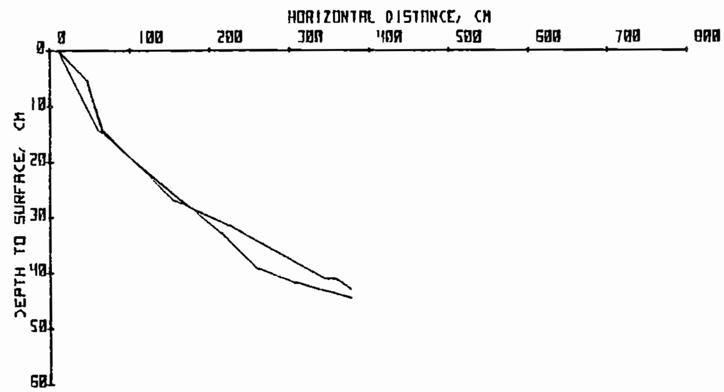

SKID TRAIL PROFILE AREA DISTURBED = -708.22 SQ CM
BULLARDS BAR
SKIDDER
HIGH MOISTURE CONTENT
STRIP NO. 1

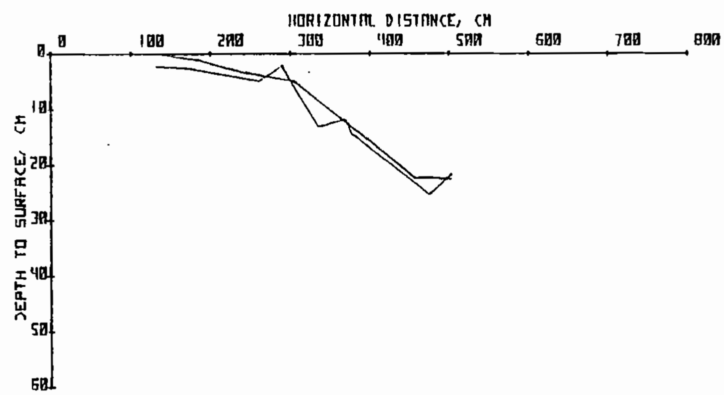

SKID TRAIL PROFILE AREA DISTURBED = 490.92 SQ CM
BULLARDS BAR
FMC-210CA
HIGH MOISTURE CONTENT
STRIP NO. 2

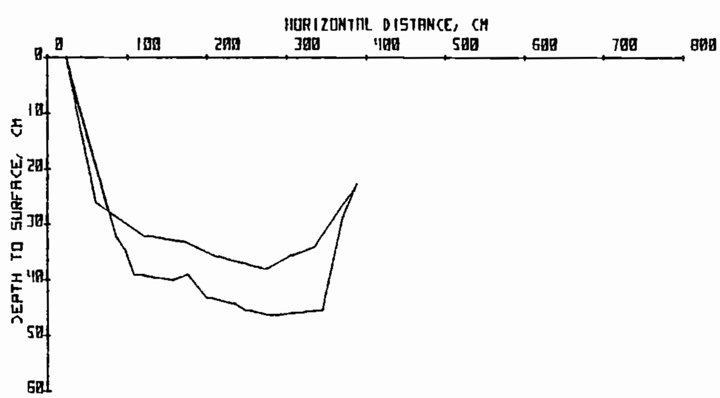

SKID TRAIL PROFILE AREA DISTURBED = 2154.965 SQ CM
BULLARDS BAR
TRACTOR
HIGH MOISTURE CONTENT
STRIP NO. 3

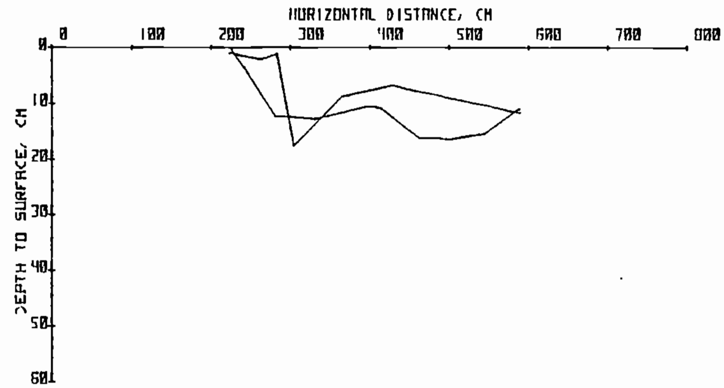

SKID TRAIL PROFILE AREA DISTURBED = 1400.885 SQ CM
BULLARDS BAR
TRACTOR
INTERMEDIATE MOISTURE CONTENT
STRIP NO. 4

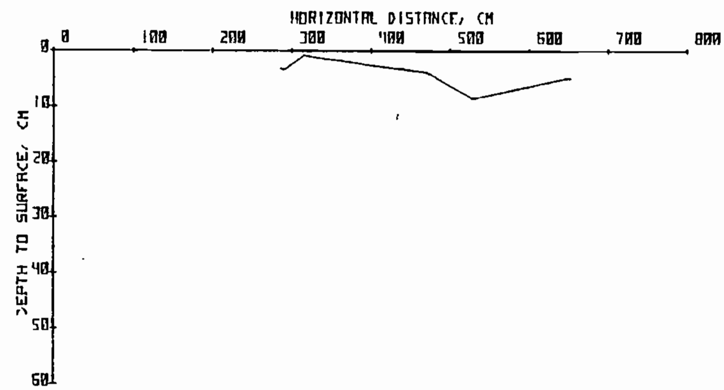

SKID TRAIL PROFILE AREA DISTURBED = 1564.765 SQ CM
BULLARDS BAR
FMC-210CA
INTERMEDIATE MOISTURE CONTENT
STRIP NO. 5

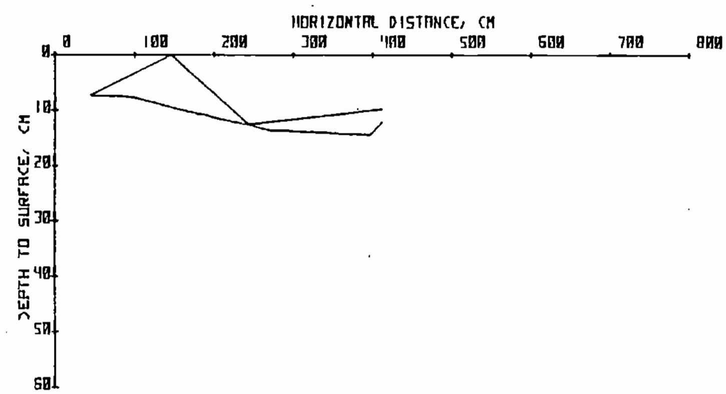

SKID TRAIL PROFILE AREA DISTURBED = 1375.615 SQ CM
BULLARDS BAR
SKIDDER
INTERMEDIATE MOISTURE CONTENT
STRIP NO. 6

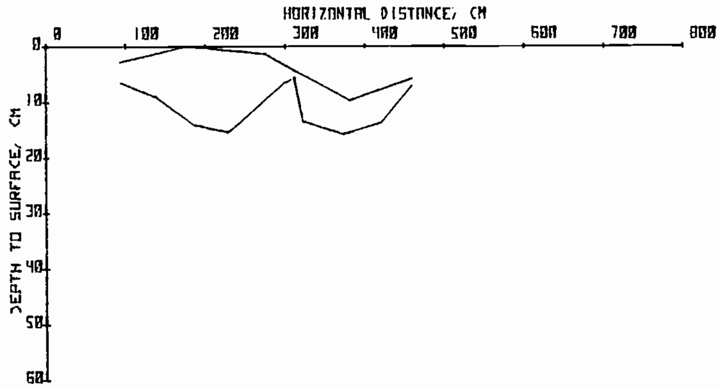

SKID TRAIL PROFILE AREA DISTURBED = 2955.31 SQ CM
BULLARDS BAR
TRACTOR
LOW (INTER) MOISTURE CONTENT
STRIP NO. 7

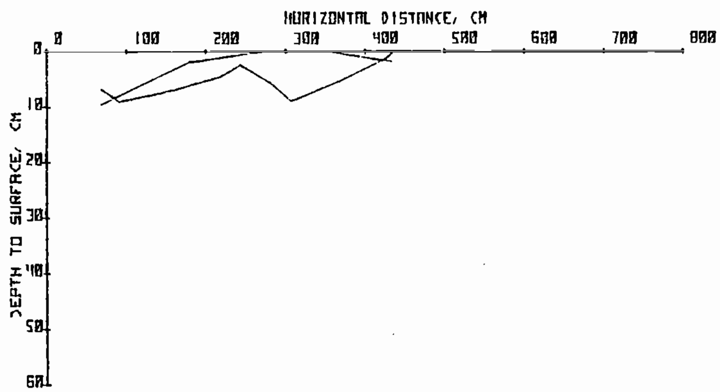

SKID TRAIL PROFILE . AREA DISTURBED = 1317.545 SQ CM
BULLARDS BAR
SKIDDER
LOW (INTER) MOISTURE CONTENT
STRIP NO. 8

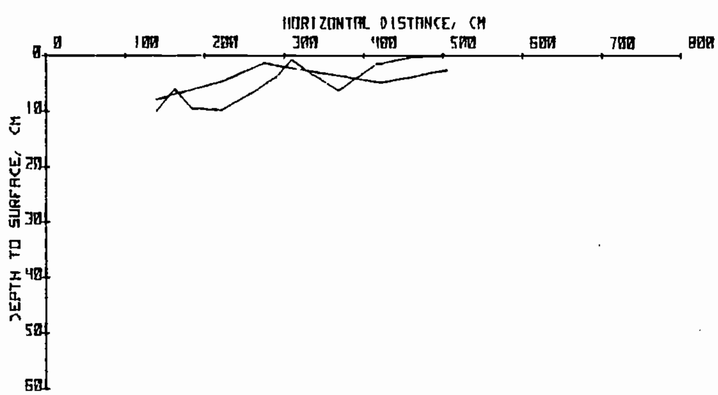

SKID TRAIL PROFILE AREA DISTURBED = 236.72 SQ CM
BULLARDS BAR
FMC-210CA
LOW (INTER) MOISTURE CONTENT
STRIP NO. 9

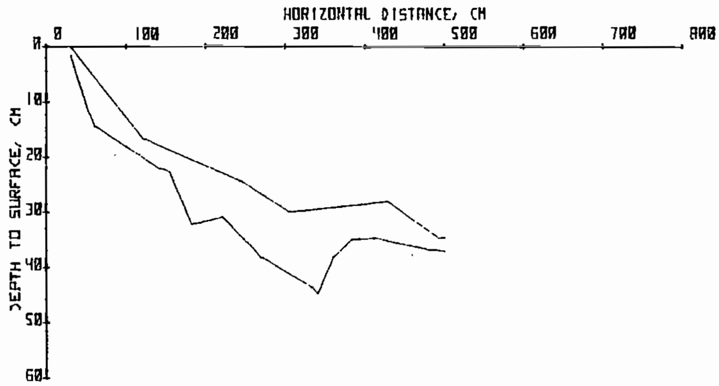

SKID TRAIL PROFILE AREA DISTURBED = 3663.3 SQ CM
PLIOCENE RIDGE
FMC-210CA
INTERMEDIATE MOISTURE CONTENT
STRIP NO. 1

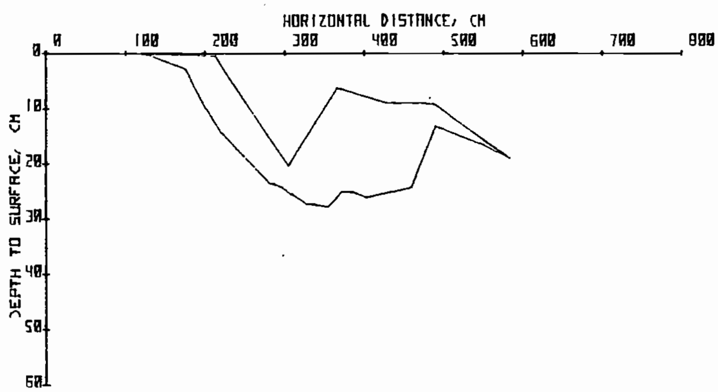

SKID TRAIL PROFILE AREA DISTURBED = 4095.02 SQ CM
PLIOCENE RIDGE
TRACTOR
INTERMEDIATE MOISTURE CONTENT
STRIP NO. 2

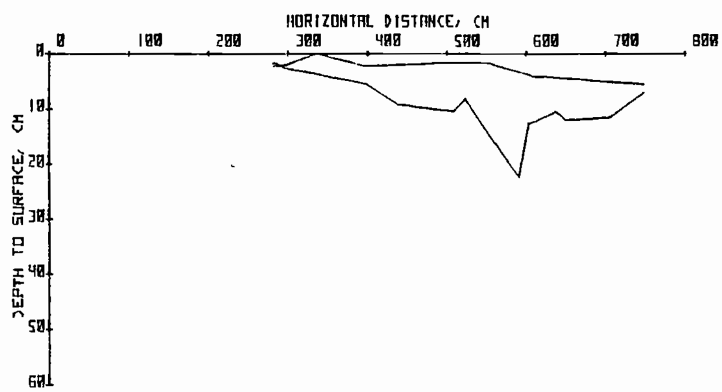

SKID TRAIL PROFILE AREA DISTURBED = 3160.305 SQ CM
PLIOCENE RIDGE
SKIDDER
INTERMEDIATE MOISTURE CONTENT
STRIP NO. 3

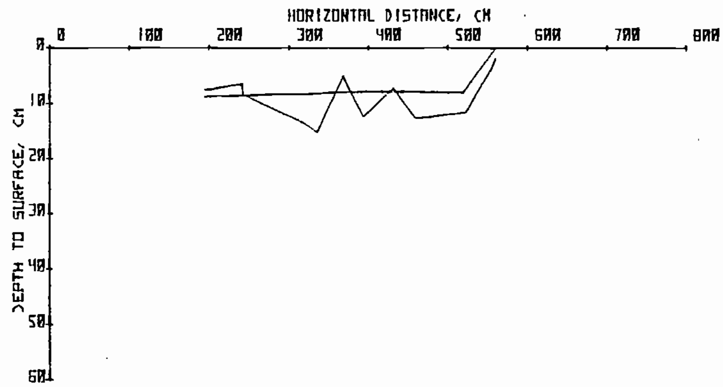

SKID TRAIL PROFILE AREA DISTURBED = 844.27 SQ CM
PLIOCENE RIDGE
FMC-210CA
HIGH MOISTURE CONTENT
STRIP NO. 4

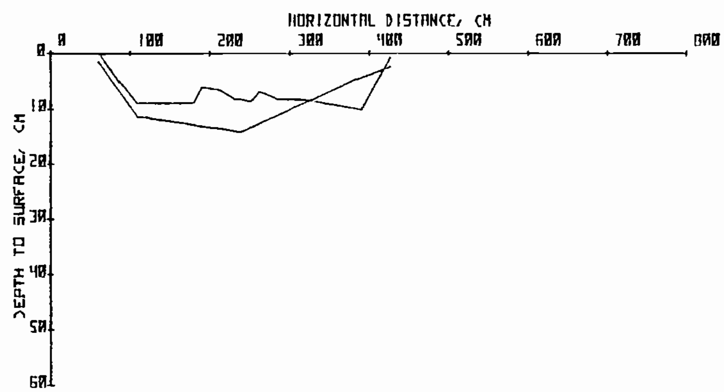

SKID TRAIL PROFILE AREA DISTURBED = -694.52 SQ CM
PLIOCENE RIDGE
SKIDDER
HIGH MOISTURE CONTENT
STRIP NO. 5

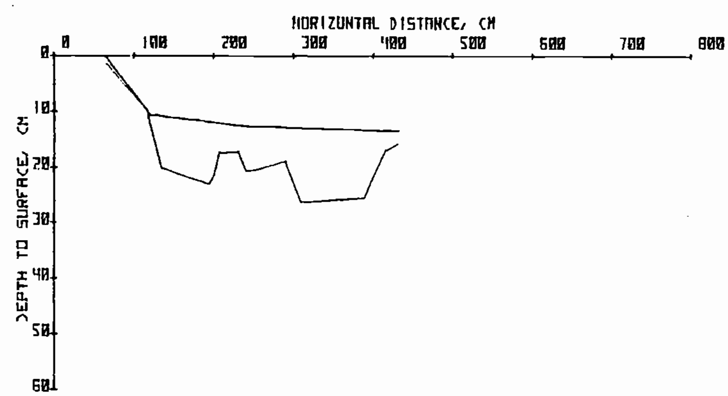

SKID TRAIL PROFILE AREA DISTURBED = 2726.515 SQ CM
PLIOCENE RIDGE
TRACTOR
HIGH MOISTURE CONTENT
STRIP NO. 6

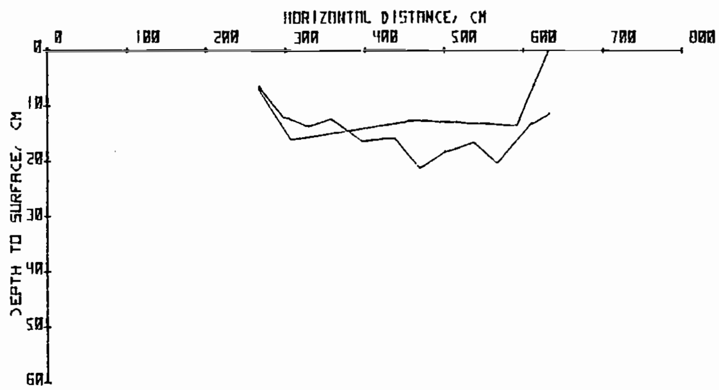

SKID TRAIL PROFILE AREA DISTURBED = 1012.205 SQ CM
PLIOCENE RIDGE
FMC-210CA
LOW MOISTURE CONTENT
STRIP NO. 7

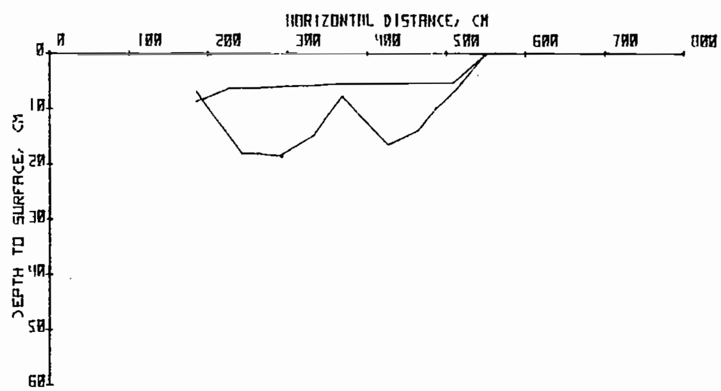

SKID TRAIL PROFILE AREA DISTURBED = 2576.56 SQ CM
PLIOCENE RIDGE
TRACTOR
LOW MOISTURE CONTENT
STRIP NO. 8

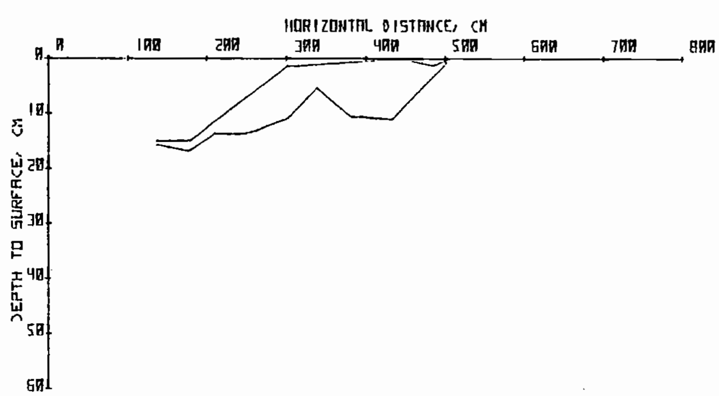

SKID TRAIL PROFILE AREA DISTURBED = 2100.895 SQ CM
PLIOCENE RIDGE
SKIDDER
LOW MOISTURE CONTENT
STRIP NO. 9

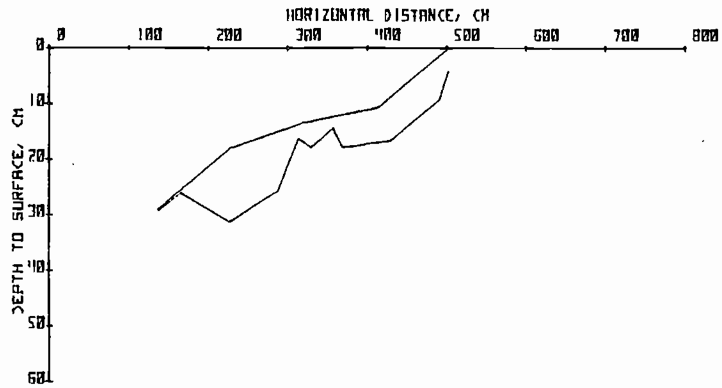

SKID TRAIL PROFILE   AREA DISTURBED = 2473.305 SQ CM
YUBA PASS
SKIDDER
LOW MOISTURE CONTENT
STRIP NO. 1

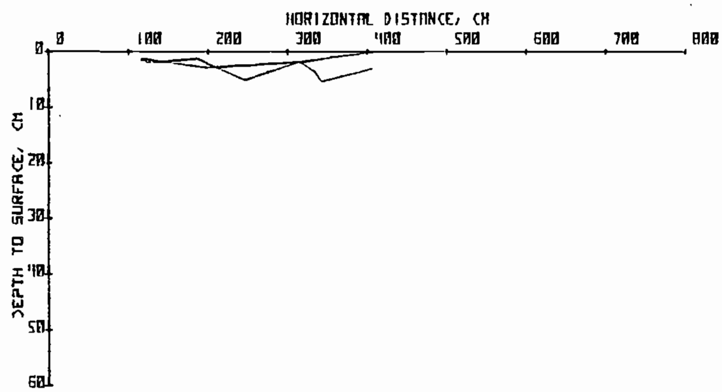

SKID TRAIL PROFILE   AREA DISTURBED = 370.895 SQ CM
YUBA PASS
FMC-210CA
LOW MOISTURE CONTENT
STRIP NO. 2

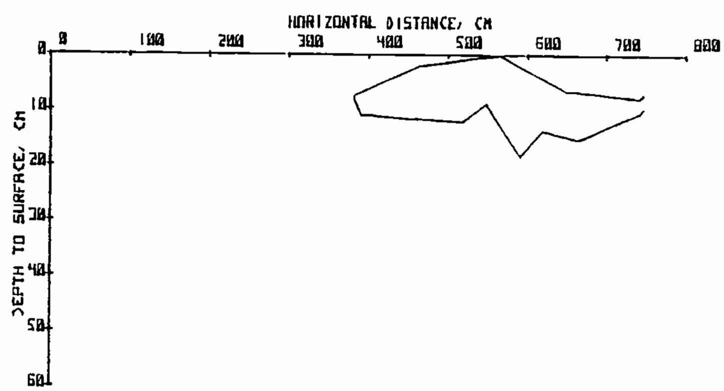

SKID TRAIL PROFILE   AREA DISTURBED = 3119.875 SQ CM
YUBA PASS
TRACTOR
LOW MOISTURE CONTENT
STRIP NO. 3

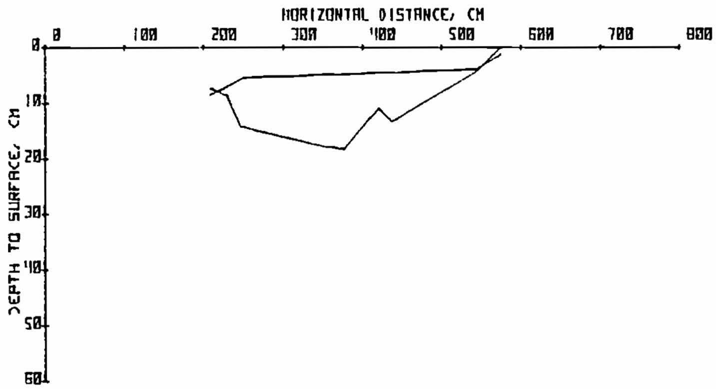

SKID TRAIL PROFILE   AREA DISTURBED = 2615.605 SQ CM
YUBA PASS
TRACTOR
INTERMEDIATE MOISTURE CONTENT
STRIP NO. 4

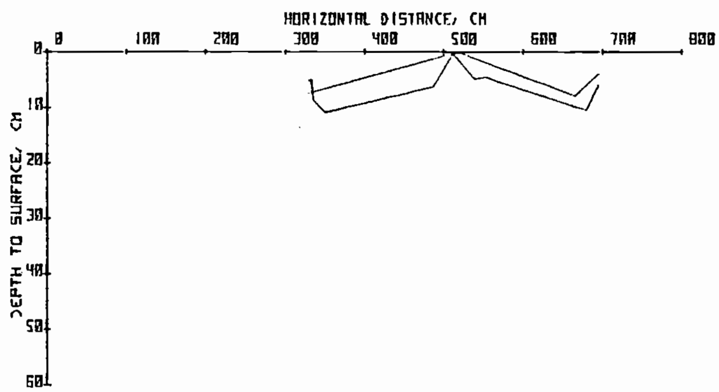

SKID TRAIL PROFILE   AREA DISTURBED = 1191.3 SQ CM
YUBA PASS
SKIDDER
INTERMEDIATE MOISTURE CONTENT
STRIP NO. 5

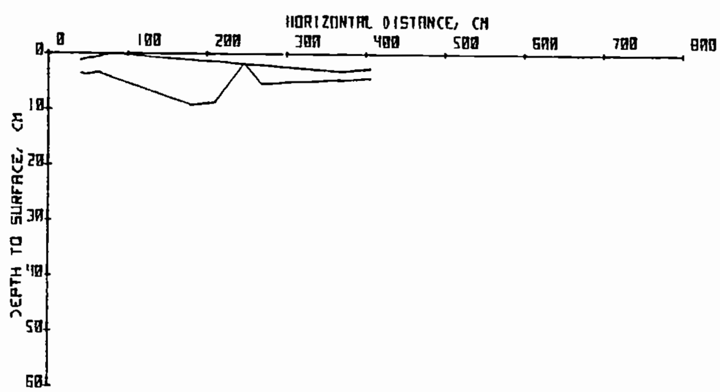

SKID TRAIL PROFILE   AREA DISTURBED = 1426.895 SQ CM
YUBA PASS
FMC-210CA
INTERMEDIATE MOISTURE CONTENT
STRIP NO. 6

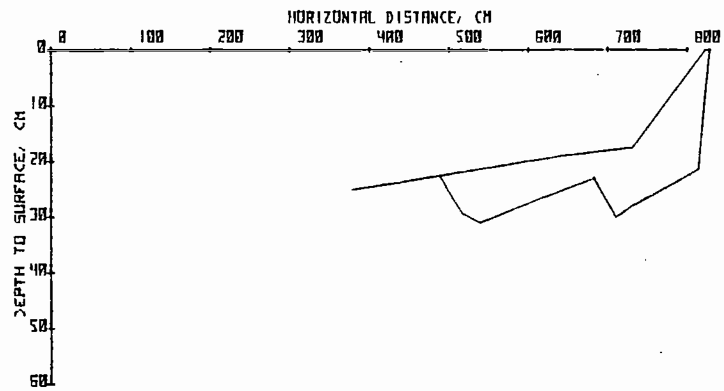

SKID TRAIL PROFILE AREA DISTURBED = 3215.025 SQ CM
YUBA PASS
FMC-210CA
HIGH MOISTURE CONTENT
STRIP NO. 7

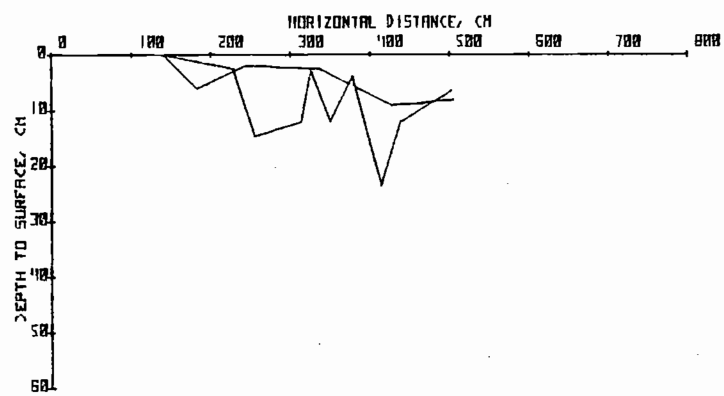

SKID TRAIL PROFILE AREA DISTURBED = 1392.875 SQ CM
YUBA PASS
TRACTOR
HIGH MOISTURE CONTENT
STRIP NO. 8

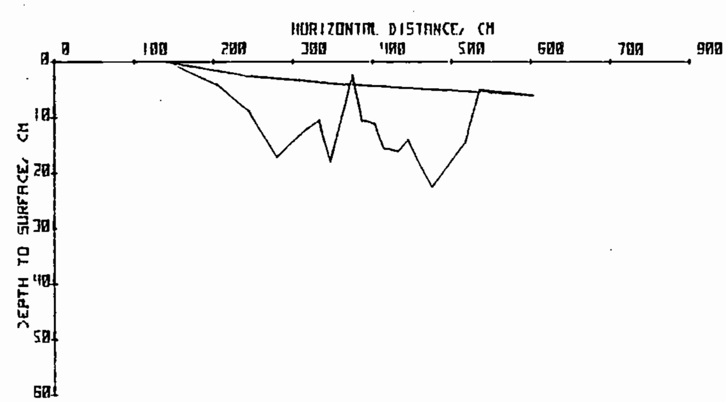

SKID TRAIL PROFILE AREA DISTURBED = 3382.775 SQ CM
YUBA PASS
SKIDDER
HIGH MOISTURE CONTENT
STRIP NO. 9